ANNUAL REVIEWS

Annual Review of Physiology

Innate Bacteriostatic Mechanisms Defend the Urinary Tract

Jose A. Munoz, Anne-Catrin Uhlemann, and Jonathan Barasch

Department of Medicine and Pathology and Urology, Columbia University, New York, NY, USA; email: jmb4@columbia.edu

Annu. Rev. Physiol. 2022. 84:533–58

First published as a Review in Advance on November 15, 2021

The *Annual Review of Physiology* is online at physiol.annualreviews.org

https://doi.org/10.1146/annurev-physiol-052521-121810

Keywords

urinary tract infection, siderophore, two component system, distal RTA, NGAL, obstructive uropathy, salinity

Abstract

Urinary tract infection (UTI) is the most common type of urogenital disease. UTI affects the urethra, bladder, ureter, and kidney. A total of 13.3% of women, 2.3% of men, and 3.4% of children in the United States will require treatment for UTI. Traditionally, bladder (cystitis) and kidney (pyelonephritis) infections are considered independently. However, both infections induce host defenses that are either shared or coordinated across the urinary tract. Here, we review the chemical and biophysical mechanisms of bacteriostasis, which limit the duration and severity of the illness. Urinary bacteria attempt to overcome each of these defenses, complicating description of the natural history of UTI.

INTRODUCTION

Scope of the Problem

UTI: urinary tract infection

NGAL: neutrophil gelatinase-associated lipocalin, also known as siderocalin or lipocalin-2

The urinary system's susceptibility to infection is illustrated by a lifetime risk of urinary tract infection (UTI), exceeding 60% in the United States (1). Some patients even have six or more infections per year (2, 3). The high incidence rate translates to an annual expense of ~US$1.6 billion for community-acquired UTI (2), and these numbers may increase further because of the emergence of broad-spectrum antimicrobial drug resistance now posing significant treatment challenges (4). Novel insights into the microbiology of UTI pathogenesis will enable alternative, antibiotic-sparing therapeutic approaches.

Definition

The definitions of pyelonephritis and UTI are obvious in general outline but are quite difficult to ascertain at the lower limit of presentation. In addition, the symptoms (e.g., pain, burning on urination) and signs (e.g., hematuria and pyuria) of these infections cannot be quantitatively compared to the bacterial burden, their virulence factors, or even the precise location of the infection within the urogenital system. A recent summary (5) of diagnostic criteria of pyelonephritis highlighted the most convincing clinical findings, including (*a*) flank tenderness or pain; (*b*) potential fever; (*c*) potential urgency, frequency, and dysuria; (*d*) pyuria and bacteriuria; and (*e*) quantitative cultures containing >10,000 colony-forming units (CFU)/mL urine (5). Although these measures, taken together, almost certainly suggest pyelonephritis, the diagnosis is uncertain when a patient presents with only some of these metrics (6), for example, if a patient lacks voiding symptoms or had an initial dose of antibiotics. In addition, the problem of diagnosis is confounded by nonspecific screening tests, utilizing dipsticks that measure the concentration of leukocytes (also a marker of kidney disease) and nitrites (that have a brief half-life and are not produced by all urinary pathogens). Perhaps clarification of the diagnosis of UTI could involve measuring bacterially induced bladder and kidney proteins (e.g., lipocalins, defensins, and RNases) that are otherwise present at low concentration in the urine. For example, urinary neutrophil gelatinase-associated lipocalin (NGAL) distinguished between UTI, colonization, and no UTI with an area under curve of the receiver operating characteristic curve (AUC-ROC) of 0.89, 95% CI (0.80–0.98) (7) by log-order changes in gene expression. NGAL distinguished active versus treated UTI and gram-positive from gram-negative UTI (8). A second problem is that most criteria for pyelonephritis also describe cystitis. Imaging may help, but these tests define only a subset of the patients suspected of pyelonephritis, such as pediatric cases with renal scaring (identified by DMSA scintiscan), obstruction (identified by ultrasound), and stones or abscess (identified by computed tomography). Perhaps the large defensin family includes members that are tissue specific, although this hypothesis is currently unsupported.

Types of Defensive Maneuvers

The urinary tract (composed of the kidneys, ureters, bladder, and urethra) deploys multilayered, intrinsic, bacteriostatic mechanisms of defense prior to the entry of dedicated immune cells. The bacteriostatic defenses draw on biophysical forces such as peristalsis and urine flow, bizarre decoy molecules, chelators that attempt to starve bacteria of nutrients, and the cellular mechanisms that alter the chemical composition of the urine. Finally, when all else fails, the infected cells are sacrificed. Every one of these mechanisms plays an essential role in restricting the severity and duration of bacterial infection.

Location, Location, Location

A critical subject, currently understudied, is the location and coordination of different defenses in different urinary organs. For example, many of the antimicrobial molecules under investigation by our lab are expressed by both bladder urothelium and pelvic and duct epithelia of the kidney. One plausible explanation for the coexpression is that urogenital organs may signal one another. For example, work from our lab demonstrated robust expression of inflammatory molecules in the kidney, even in a cystitis model of infection (C57BL6 mice). These mice have no demonstrable reflux of luciferase-expressing bacteria, and bacteria were not cultured from the kidney (**Figure 1**). We hypothesized that circulating cytokines released by the infected bladder induced inflammatory molecules in the kidney. While still a viable hypothesis, given that the bladder secretes cytokines such as granulocyte-macrophage colony-stimulating factor (GM-CSF), interleukin 6 (IL-6), IL-8, keratinocyte-derived chemokine (KC) (9–11), and C–C chemokine ligand 2 (CCL2), sensitive polymerase chain reaction (PCR) directly from kidney sections (K. Xu, T. Shen, M. Werth, A. Levitman, J. Barasch, unpublished data) revealed the presence of bacterial DNA, perhaps likely due to reflux of small numbers of nonviable bacteria failing to reach culture threshold. This finding provides a simple mechanism that can coordinate bladder and kidney host responses even without overt infection of the kidney. In this view, cystitis is not an isolated disease localized to the bladder, but rather a systemic illness that induces gene expression in the kidney. Perhaps coordination between the kidney and bladder is promoted by the expression of transcription factors downstream of these signals. Tfcp2l1 controls the differentiation of principal and intercalated cells (ICs) from a bipotential double positive or transitional cell type (12, 13) in the collecting ducts. Bladder urothelium also expresses Tfcp2l1. In summary, approaches examining multiple urinary organs are required to investigate the coordinated defense against UTI and to determine whether the coordination optimizes the expression of antimicrobials throughout the urinary tract.

IC: intercalated cell

The location of the infection and the expression pattern of antimicrobial responses should be compared. While well established in bladder urothelium (11), the natural history of bacterial infection in the kidney is uncharted. Bacteria are known to localize initially to the collecting

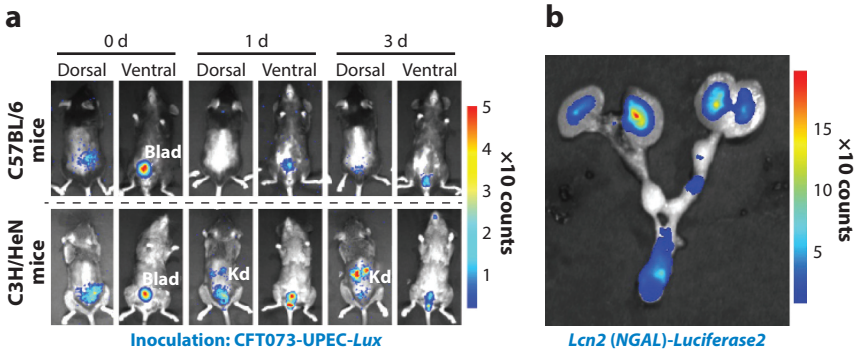

Figure 1

(*a*) C57BL/6 (nonrefluxing) and C3H/HeN (refluxing) mice were inoculated with CFT073-UPEC-*Lux*. Mice were imaged on both the dorsal and ventral sides. Note that UPEC-*Lux* remained in the bladder (Blad) of C57BL/6 mice (cystitis model), but ascended to the kidney (Kd) in C3H/HeN mice (pyelonephritis model). (*b*) Although the C57BL/6 kidney is culture negative, inoculation with CFT073 activated *Lcn2* (*NGAL*)-*Luciferase2* in the pelvis and medulla of the kidney, demonstrating that cystitis activates gene expression in the kidney. Figure adapted with permission from Reference 8. Abbreviation: UPEC, uropathogenic *Escherichia coli*.

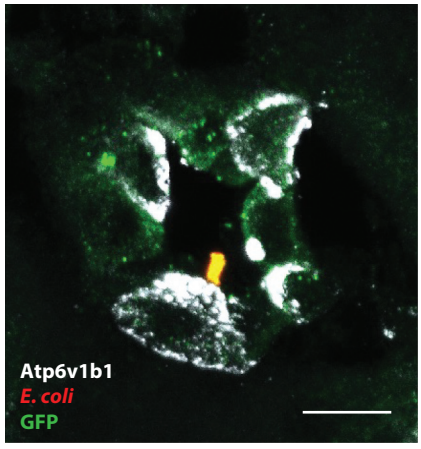

Figure 2

Inoculation of C3H/HeN mice with UTI89-GFP *Escherichia coli* demonstrated the distribution of bacteria in the collecting ducts and anchorage at the surface of an intercalated cell. *E. coli* were identified by both green fluorescent protein (GFP) fluorescence and immunostaining with *E. coli* antibody (*yellow*). Intercalated cells were identified by immunostaining for Atp6v1b1 (*white*).

ducts where they may associate with ICs preferentially (8, 14, 15) (**Figure 2**). However, a recent study showed that the bacterial receptors, glycosphingolipid and mannosylated glycoproteins, are present throughout the collecting duct (16), implicating the spread of bacteria from the surface of ICs to surrounding principal cells (16). Bacteria may then traverse the epithelial layer in a Toll-like receptor 4 (TLR4)- and lipid-raft-dependent fashion (17). Alternatively, the expression of virulence factor α-hemolysin (HlyA) and the cytotoxin Sat results in the disruption of tight junctions and the paracellular passage of bacteria into the interstitium (18). Other investigators have found that bacteria can arrive in the cortex of the kidney even soon after infection (19). These new data have identified pathways of bacterial arrival in the kidney, but thereafter the natural history of dispersal of bacteria has not been carefully tracked. Although HlyA has been found to be necessary for the spread of bacteria beyond the urogenital tract (20), even the source of bacterial urosepsis is unknown, but it presumably involves migration of bacteria from the collecting duct into lymph or venous blood (e.g., the medullary vasa recta or cortical peritubular capillaries). New inquiries are needed to compare the evolving location of infection with the evolving location of the epithelial response.

In summary, although many types of defenses have been identified, their locations and coordination between different urogenital organs have not been mapped. Readily available tools for spatial transcriptomics will help. For example, our lab has adapted a cell- and time-specific method of isolating RNA without the need for tissue or cell dissociation, fluorescence activated cell sorting, or other destructive measures. The technique utilizes acute labeling of nascent RNA with thio-uracil at the time of choosing after the initiation of UTI, and in a cell-type-specific manner by activating a phosphoribosyl-transferase with Cre recombinase (T. Shen, J. Stauber, K. Xu, A. Jacunski, N. Paragas, et al., unpublished manuscript). A second method for spatial localization is based on the genetic response of tubule epithelial cells to the kidney's cortical-medullary osmotic gradients (21). The same requirement to localize bacteria applies to the natural history of pyelonephritis, particularly given that bacteria associate with different nephron cells in entirely different chemical/osmotic environments during infection. Bacteria encoding luciferase or physiological beacons (22) can help with localization. Perhaps these inquiries will demonstrate that

HlyA: α–Hemolysin

unique antimicrobial mechanisms accommodate the continuous flow of urine in the upper tracts compared with hours-long stasis in bladder.

UPEC: uropathogenic *Escherichia coli*

INVADERS FROM THE INTESTINE

Escherichia coli is by far the most common cause of acute UTI. Other Enterobacterales, in particular *Klebsiella* spp. (~7%) and *Proteus* spp. (5%), contribute to the burden of UTI. Other organisms such as *Pseudomonas aeruginosa*, *Enterococcus faecalis*, *Streptococcus bovis*, and the fungus *Candida albicans* contribute to UTIs, particularly in the healthcare setting (23–25). However, the vast majority of infections are caused by uropathogenic *E. coli* (UPEC).

UPEC are characterized by a unique set of virulence factors encoded on four phylogroups (A, B1, B2, D) of pathogenicity islands, harboring adhesins, toxins, surface polysaccharides, flagella, and iron-acquisition systems. Years of research have established that these molecular factors uniquely enable UPEC to first colonize the urethra, ascend into the bladder lumen, and subsequently adhere to the surface of the bladder and kidney epithelia via chaperone–usher pathway (CUP) pili, such as the type 1 pilus containing FimH. Adherence is followed by biofilm formation, invasion, and replication by forming bladder intracellular bacterial communities. These are quiescent intracellular reservoirs growing in the underlying urothelium. Much less is known about the sequence of infection in the kidney.

UPEC have unique properties to form a colonizing reservoir in the gut preceding urinary colonization. Spaulding et al. (26) systematically deleted each CUP operon present in the model UT189 UPEC isolate. This revealed that the *fim* operon (encoding type 1 pili) and *ucl* pilus operon (encoding F17-like pili) were key contributors to gut colonization. When both were deleted, colonization was even further decreased, suggesting that they serve nonredundant roles in gut colonization. Importantly, the deletion of *ucl* did not impact the severity of bladder infections, defining its primary role in gut colonization. An important role for type 1 fimbriae in gut colonization was supported by studies by Sarkar et al. (27) in ST131 EC958.

The binding of UclD was visualized in the lower portion of colonic crypts, whereas FimH bound to the upper region. Molecular correlates suggested that these pili promote binding of UPEC to different carbohydrate structures. Interestingly, the F17-like pili *ucd* is structurally related to F17-like pili from enterotoxigenic *E. coli*. Moreover, it was mainly present in the B2 phylogroup and was frequently described in UPEC isolates from women with recurrent infections. As a proof-of-principle that these molecular features can be leveraged for treatment, oral exposure of mice to a mannose M4284 (specific for FimH) significantly reduced colonization with UPEC in the gut, bladder, kidneys, and urine. Novel nonantibiotic-based treatment modalities will be increasingly important given the increasing emergence of both fluoroquinolone- and extended-spectrum beta-lactamase resistance in the global multilocus sequence type UPEC lineage ST131.

Despite potential differences in clinical presentation between lower and upper urinary tract infections, our understanding of microbial molecular determinants of these disparate infections remains limited. Biggel et al. (28) leveraged genome-wide association and phylogenetic approaches. The authors took advantage of a well-curated collection of over 900 isolates, separated into groups of severe UTI (i.e., pyelonephritis or urinary-source bacteremia) compared with noninvasive UPEC, defined as isolates associated with asymptomatic bacteriuria or bladder infection (cystitis). The P fimbriae–encoding papGII locus was the key feature distinguishing invasive UPEC. Further, multiple invasive UPEC lineages emerged, probably through the repeated horizontal acquisition of diverse papGII-containing pathogenicity islands. Future studies might identify patients at risk for more invasive disease by applying these molecular findings to urinary isolates.

CHEMICAL BARRIERS: URINE IS POISONOUS

Chemical Decoys

dRTA: distal renal tubular acidosis

NKCC2: Na-K-Cl triple cotransporter

UPEC bind to glycosylated membrane proteins to establish anchorage and initiate the infection (29). In turn, mammalian cells take advantage of bacterial tropism by secreting decoys, which mimic the binding site (30). Uromodulin serves as a decoy because it presents mannose residues. It has two high mannose N-glycan sites, one of which was directly visualized by cryo-electron tomography binding to FimH, the adhesin in type I piliated UPEC. Binding could be blocked with excess mannose. Consistently, urine uromodulin reduced the incidence of human UTI (31) and, conversely, the knockout of uromodulin increased mouse susceptibility to UTI (32). Accordingly, the removal of the critical mannose residues suppressed the bacterial-binding activity of uromodulin (33). It is likely that the high mannose site is exposed by proteases at the cell surface (34). Hence, the first step in defeating colonization by gut organisms is to block bacterial binding to epithelia, surprisingly including mannosylated desmoglein-2 (16) in the collecting duct.

Acidity

UPEC that are not entrapped and expelled in the urine by filamentous uromodulin confront acidified urine, which represents a key bacteriostatic defense that suppresses the growth of gram-negative *E. coli* and *Klebsiella*. These data were first published in the *Journal of Urology* in 1917 (35) and have been confirmed in principle using many additional organisms, even gram-positive *Staphylococcus saprophyticus* (36).

Consistent with these findings, suppression of acidification is associated with more frequent or more severe infections. For example, children with urinary reflux come to medical attention because of repetitive urinary infections with *E. coli* (89%), *Klebsiella pneumoniae* (3%), and *Proteus mirabilis* (2%) (37). Half of these patients demonstrate urinary alkalinization, accompanied by systemic acidosis in association with interstitial infiltrates, kidney scarring, and fibrosis (38, 39). In these patients, urine did not maximally acidify during ammonium loading, the urine anion gap remained positive, and bicarbonaturia was found. This disturbance is called a distal renal tubular acidosis (dRTA) consistent with malfunction of the collecting duct ICs.

Similar to vesiculo-ureteral reflux, obstruction also predisposes to UTI and is accompanied by apparent dRTA, defective ammonium excretion, and a positive anion gap (40) in as many as 50% of infants with unilateral or bilateral hydronephrosis. Similar data were obtained in mice, rats, dogs, and nonhuman primates exposed to different obstructive methodologies. Indeed, autopsy specimens of human and nonhuman primate neonates demonstrated that the number of ICs varied inversely with the degree of duct dilation, reducing the number of ICs in the obstructed kidney by two-thirds (41). Similar data were obtained in a postnatal unilateral ureteral obstruction model (42). Nielsen's group (43) found that multiple acid base transporters were reduced during 24 h of obstruction, including transporters in the proximal tubule (NHE3, NBCe1) and transporters in the thick ascending limb of Henle (TALH) and collecting ducts such as the Na-K-Cl triple cotransporter NKCC2 and the H^+-ATPase, identifying a response throughout the nephron, even though the dRTA phenotype dominated. Surprisingly, even brief obstruction caused persistent (>4 days) downregulation of NKCC2 and H^+-ATPase in the inner strip of the outer medulla and in the inner medulla displaying persistent impairments of H^+ secretion (lasting >4 days) (44). Even when outer medullary collecting tubules were extracted and microperfused or when membrane vesicles were analyzed, defective H^+ secretion persisted, implying a prolonged defect in ICs (45). A cell autonomous defect was also shown by Gluck's group (46), who found that brief obstruction inhibited the apical positioning of H^+-ATPase and that prolonged obstruction led

to the loss of these cells altogether, particularly in the outer medulla. All of these entities share a strikingly reproducible phenotype, linking UTI with flow abnormalities and defects in ICs.

Although the association of H^+ physiology and repetitive UTIs is a compelling correlation, the chance identification of the transcription factor Tfcp2l1 by our lab strengthened the association. Deletion of *Tfcp2l1* (8) prevented the development of ICs and at the same time resulted in higher colony counts throughout the urinary system. Given that only ICs can reduce urine pH sufficiently to achieve bacteriostasis, these data explain why patients with distal renal tubular acidosis are at risk for urinary infections (47).

Ent: enterochelin

There are many reasons why acidification can suppress microbial growth. It has been found that the transcription of bacterial adhesive fimbriae is suppressed (48) by acidification. In addition, the antimicrobial peptides cathelicidin and the defensins are upregulated in collecting duct cells by acidification (49). But perhaps an even stronger observation is that while urine H^+ suppresses *E. coli*, urine alkalinization positively selects for other pathogens. In a 14-year retrospective cohort study of 5,201 patients, urine pH 8 was associated with growth of *P. mirabilis* and *P. aeruginosa* in 25% of children older than 12 months (50). Each of these examples supports the notion that urine pH is a determinant of UTI and indicates an important area of ongoing research.

Starvation: Nutritional Immunity

Starvation is a second mechanism that limits the growth of UPEC. Although iron is the fourth most common element in the Earth's crust and is abundant in mammalian cells, iron's chemistry prevents direct transfer across aqueous spaces. This is because the common oxidized form of iron, called ferric iron, is insoluble in water (51) (Ksp = 10^{-9} M), particularly in phosphate solutions (Ksp = 10^{-13} M) (51), whereas in its reduced form, ferrous iron is unstable and decays into ferric iron with the production of toxic hydroxyl radicals. As a result, iron must be shepherded by specialized carriers. Mammals use high-affinity proteins (e.g., transferrin; 10^{-20} M) and organic molecules [e.g., heme, citrate, catecholates (52)] to solubilize and deliver iron. Nutritional immunity (53) is the concept that mammals suppress the growth of bacteria by chelating iron. In turn, microbes must outcompete mammalian chelators to claim iron from limiting sources [urine: mouse = 0.8 μM, human = 0.7 μM (8)].

Genome-wide and targeted screens have repeatedly demonstrated that bacterial virulence depends on expressing specialized tools to capture iron. To steal our iron, bacteria produce siderophores, which are organic molecules (54) with astronomical affinity for ferric iron [e.g. enterochelin ~$K_a = 10^{50}$ (55)]. The most impressive and widespread are the catecholates, such as enterochelin and its relatives, salmochelin, bacillibactin, agrobactin, corynebactin, fluvibactin, and vibriobactin, all of which utilize six catechol hydroxyl groups to supply electrons to the partially filled orbitals of iron. Even simplifications and fragments of these siderophores, such as monomeric catechol, 2,3 dihydroxybenzoate, pyrogallol, and 3-methyl catecholate, are partially competent siderophores (52, 56). The iron-loaded siderophores are recaptured by cognate receptors (57) [Iha and FepA for Ent:Fe; IroN for salmochelin (58)], which *E. coli* upregulate upon infection of mouse or human urinary tracts.

It is conceivable that the mammalian urinary system can overcome the *tris*-catecholate siderophores with acidified urine. Protonation of the hydroxyl groups reduces affinity of Ent for Fe by converting catecholate into salicylate mode binding, which in turn may promote iron release (51). If acidification was effective, iron lost into the urine would bind to pH-insensitive lactoferrin. Rather, the kidney and bladder have devised an entirely novel mechanism to overcome the catecholate siderophores. Roland Strong and colleagues (59) identified that a mammalian protein called NGAL, also known as lipocalin 2 or siderocalin, bound the catecholate siderophore

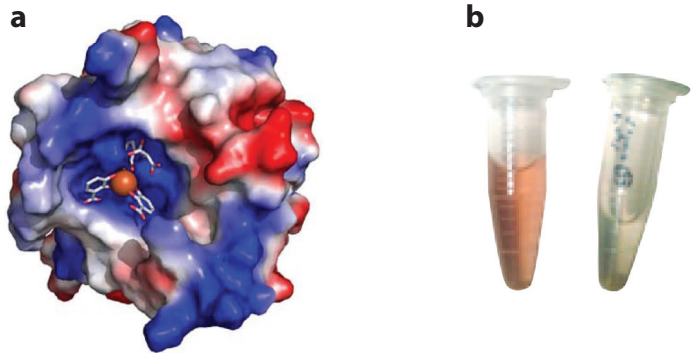

Figure 3

(*a*) Neutrophil gelatinase-associated lipocalin (NGAL; lipocalin 2 or siderocalin) with bound siderophore 2,3 dihydroxybenzoic acid. Iron is indicated by the red sphere. Crystal structure solved by R. Strong, Fred Hutchinson Cancer Research Center, Seattle, Washington. Photo provided by R. Strong. (*b*, *left*) The NGAL:siderophore:Fe complex generates a red color that is stable for years even with repetitive washing. (*b*, *right*) NGAL:siderophore is colorless.

Ent. The affinity of NGAL for Ent was subnanomolar and was resistant to low pH. Indeed, the NGAL:Ent:Fe complex maintains its red coloration at pH 4.5 for many years (**Figure 3**). The interaction of Ent with NGAL suppressed bacterial growth and induced gene activation in bacteria, mimicking the application of the medicinal iron chelator, DFO (**Figure 4**). Hence, NGAL caused bacterial iron starvation and bacteriostasis. Suppression of bacterial growth can be demonstrated in vivo by inoculating mice with a mutant form of NGAL that bypasses megalin-based capture mechanisms in the proximal tubule and enters the urine. Consequently, K3Cys mutant NGAL may be useful to augment nutritional immunity (60). Conversely, in mouse NGAL knockout models, clearance of urinary infection was delayed. Hence, bacteria steal our iron, and we steal its siderophores (61).

An additional type of siderophore can also bind to NGAL: Urine contains nonsulfated catechols (1–10 μM) that can occupy the internal cavity of NGAL and dock iron by forming a quaternary complex at subnanomolar affinity (52). The chelation of iron is a terminal reaction when bacterial Ent is available (NGAL:Ent:Fe is pH insensitive), but it is reversible when the pocket is occupied by catechols (NGAL:Catechol:Fe dissociates <pH 6.3) (52, 59, 62, 63). NGAL:Catechol$_3$:Fe can serve as an iron transport protein, but in the setting of urinary infection in the acidified urine, the catechol metabolites are replaced by Ent.

NGAL differs in many respects from the cathelicidins, defensins, and RNases (64). NGAL (urine 20 ng/mL) is intensely upregulated in patients by tubular and tubulointerstitial damage (urine up to ~5,000 ng/mL) (65, 66), particularly when associated with infection, sepsis, or urosepsis. In fact, the presence of urinary NGAL in neonates—at the time of first clinical suspicion—predicted which blood cultures would grow pathogenic bacteria and which would not (67). In mice, cecal ligation and puncture models produced a 531-fold increase in kidney NGAL. UTI in humans with gram-negative organisms induces NGAL expression, which was reversible with antibiotics. In the setting of acute tubular injury (ATI) of the kidney of any cause in humans or mice, urinary NGAL (uNGAL) levels may rise 10–100 fold.

To evaluate the sources of uNGAL, we created a NGAL-*Luc2-mCherry* reporter mouse to continuously detect NGAL in real time in whole-body scans (68). We evaluated ischemia-reperfusion, systemic sepsis, and more recently, UTI. Ischemia-reperfusion induced reporter expression within 3 h: NGAL bioluminescence and uNGAL were proportional to the intensity of the stimulus and

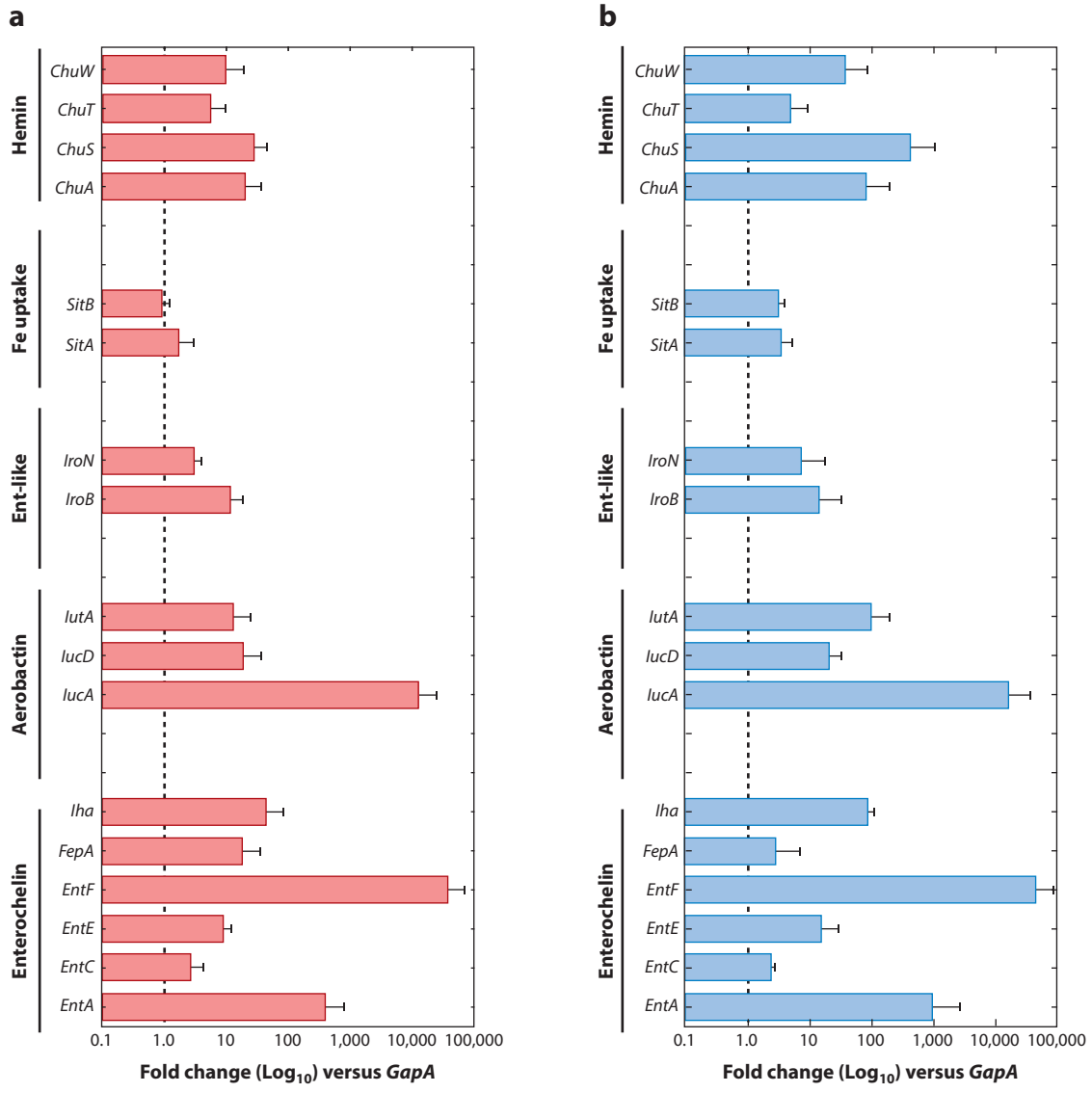

Figure 4

(*a*) Addition of neutrophil gelatinase-associated lipocalin (NGAL; lipocalin 2 or siderocalin) to uropathogenic *Escherichia coli* (UPEC)-stimulated bacterial iron gene expression. (*b*) Addition of DFO, the medicinal iron chelator, stimulated the same bacterial iron gene expression. Figure adapted with permission from Reference 8.

identical in timing to the appearance of NGAL protein in the urine. NGAL bioluminescence originated in the kidney medulla and in situ showed that TALH and collecting ducts expressed NGAL. ICs consistently expressed NGAL when mice were treated with Gram-negative lipopolysaccharide (LPS), but few if any responses were generated by treatment with Gram-positive Pam3C. In fact, medullary cells isolated from NGAL reporter kidneys responded to UPEC by expressing NGAL, and conversely, antibiotics squelched NGAL induction. In short, bacteria/ligands activate NGAL expression. In human kidney biopsies, NGAL expression was more widespread than

in mouse, occupying the entire collecting duct, and in the case of severe injury, the proximal tubule as well. Taken together, crystal structure, biophysical measurements, mouse knockouts, and in vitro growth assays demonstrate that NGAL is a bacteriostatic agent utilizing cognate recognition of an organic molecule originating from bacteria. NGAL differs from other antimicrobials in its limited expression at baseline, its intensive induction by both septic and aseptic tissue damage, its mass amount in urine (1–10 μM), and the specificity of its targeting (nonglycosylated catecholate siderophores).

Finally, it should be noted that urinary and serum NGAL may be coexpressed, but human serum NGAL forms large heterogeneous disulfide binding complexes (>100 KDa) (69, 70) of unclear relevance to urinary defense.

More than Ent

The characteristics of NGAL provided additional insights into infection by urinary bacteria. Although many of the catecholate siderophores listed above can be decommissioned by NGAL, serving as a catecholate-specific decoy receptor (52, 59), urinary *E. coli* overcome the NGAL blockade by glucosylating Ent, creating salmochelin, a stealth siderophore that cannot bind NGAL (71). *E. coli* also benefit from synthesizing noncatecholate siderophores [e.g., the hydroxamate aerobactin (*IucABCD* genes) and carboxylate yersiniabactin (*Ybt* genes) (72)] that target distinct receptors [*IutA* and *FyuA* for aerobactin and yersiniabactin, respectively (73)]. Indeed, sampling urinary bacteria collected from patients demonstrated the extensive diversity of iron capture mechanisms. Examples range from uniquely Ent^{+ve} bacteria (NR4685, NR7715) to complex strains such as UTI89 that encode many iron and heme capture pathways (e.g., heme receptors: ChuA^{+ve}, Hma^{+ve}; siderophore receptors: Ent^{+ve}, FyuA^{+ve}, IroN^{+ve}, IroB^{+ve}, SitA^{+ve}, and SitB^{+ve}) (**Figure 5**). In short, each urinary infection differs in the mechanisms of iron capture.

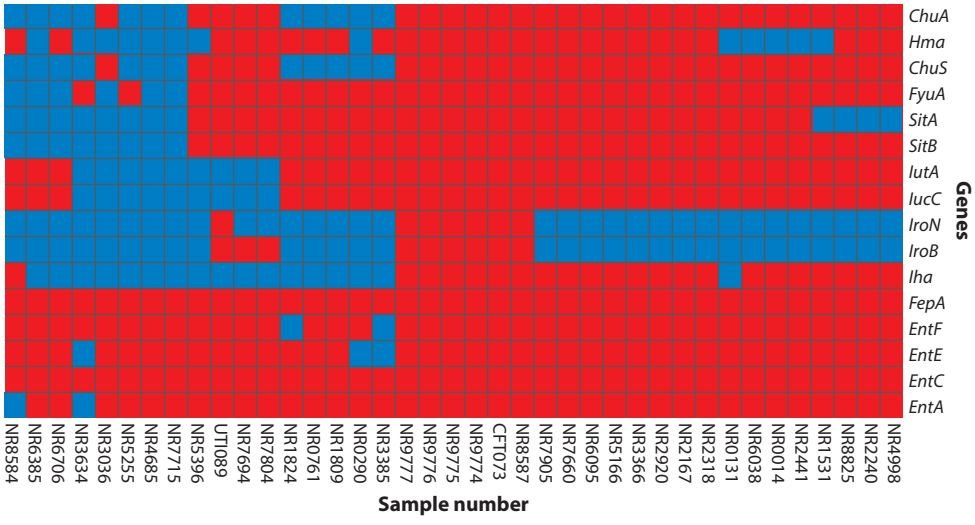

Figure 5

The genetic diversity of urinary bacteria: a sampling of urinary bacteria collected from patients, sequenced and biobanked at Columbia University by the Microbial Genomics Biomedical Core. The heat map demonstrates the extensive diversity of iron capture mechanisms employed by bacteria infecting different patients. Examples range from uniquely Ent^{+ve} bacteria (NR4685, NR7715) to complex strains such as UTI89 that encode many iron capture pathways (heme receptors: ChuA^{+ve}, Hma^{+ve}; diderophore receptors: Ent^{+ve}, FyuA^{+ve}, IroN^{+ve}, IroB^{+ve}, SitA^{+ve}, and SitB^{+ve}).

An important note concerns the relative worth of a specific siderophore type. Some data suggested that Ent was not essential for the pathogenesis of UTI, as other siderophores could compensate for Ent deletion. However, prior to our report (8), it was not known that Ent was already auto-inhibited by uNGAL. Hence, Ent deletion was not contextualized because the urothelial response to infection was unknown (54, 72, 74, 75). In summary, the data show that rather than expressing a hierarchy of siderophores, each infection expresses a different multiplicity of iron transport pathways. Indeed, enterochelin^{-ve}/aerobactin^{-ve} bacteria are still viable, implying alternatives to iron transport.

Heme

An alternative to ferric iron:siderophore biology is ferrous iron:heme biology. Evidence for the heme system includes the following. (*a*) Uropathogenic *E. coli*, including commonly studied CFT073 and UTI89 (76) and most clinical urinary isolates, produce HlyA, a virulence factor (77), which kills urothelium and lyses red blood cells (78, 79). (*b*) The American Urological Association (80) reports that normal urine contains ~3 million cells/day (the Addis count) (81, 82), potentially providing iron (3×10^{15} atoms/day) adequate to support the growth of 3×10^{10} bacteria (83). In fact, UTI further upregulates hematuria (3- to 5-fold) (84). (*c*) Hemoglobin, haptoglobin bound with iron, and heme are found in postinfectious urine (85–87). (*d*) Heme can be captured from these proteins by secreting an equivalent of a siderophore, called a hemophore [HasA and related Hux and Hus (88, 89)]. *E. coli* instead directly capture heme bound to hemoglobin, haptoglobin, and albumin using two high-affinity receptors (90, 91) called ChuA and Hma. (*e*) We confirmed that ChuA-Hma double mutants (92) and Hma single mutants (93) are growth restricted (90) and respond poorly to exogenous heme, while conversely, wild-type bacteria respond to urinary hemoglobin/heme (from phenylhydrazine lysis of RBC). In summary, UPEC grow in the presence of urinary RBC and hemoproteins.

Downstream of ChuA and Hma are complex machines that liberate iron from heme. Heme is driven across the periplasmic space by the energy-transducing TonB, ExbB, and ExbD (91) complex. In *E. coli* (94), the traffic is assisted by heme-binding protein ChuT, permease ChuU, and ATP-binding ChuV (95). Heme is then captured by cytochromes or destroyed by hemoxygenases [HemO (96), HmuO (97), cyano-HO-1, HO-2 (98), and PigA/BphO (99)]. *E. coli* heme oxygenase ChuS binds heme rings, accepts reducing equivalents, and releases fragments of heme (hematinic acid and tripyrroles) (100–102). ChuS-deleted (103) bacteria, like other HO knockouts, are unable to use heme as an iron source (96) and are not competitive in growth assays. ChuS homologs are found in many other heme-utilizing bacteria, including ShuS [*Shigella* (91, 104)], EhuS (*Enterobacter*), HemS (*Yersinia*), and BhuS (*Bordetella*). ShuS and ChuS were reported to be upregulated by iron deficiency.

The operation of bacterial heme metabolism can be directly observed by detecting the release of two metabolic products with potentially opposing effects. While the release of iron from heme supports bacterial growth, and at low levels, the release of carbon monoxide (CO) can serve as a signaling molecule (103), higher levels of CO (105) abolish the growth of new bacterial colonies and stunt the growth of established colonies (105). Electron paramagnetic resonance studies demonstrated that after 10 min of CO exposure, total cell iron decreased by 50% and, in response, *Ent* synthetic genes were upregulated 30-fold via *fur* regulation (106). These data demonstrate a potential limit of the heme nutrient pathway (CO toxicity) and that heme metabolism can cross talk with iron siderophore pathways.

DNA sequencing and acute transcriptomics of bacteria recovered from the urinary tract identified the principle that urinary bacteria utilize varying combinations of heme and ferric iron

transport. Two-dimensional polyacrylamide gel electrophoresis and tandem mass spectrometry (107) demonstrated prominent and consistent upregulation of heme transporters ChuA and Hma and variable expression of catecholate siderophore receptors IroN, Iha, and FepA. In two different cross-sectional studies, Hma and FyuA (yersiniabactin receptor) were most prominently upregulated in patients with cystitis with lower urinary tract symptoms (LUTS) compared with the same bacteria in the same patient's stool, whereas IutA predominated in those with pyelonephritis (108, 109). In colonizer *E. coli*, ChuA, IutA, FyuA, and FepE were upregulated compared to the same strain grown in the urine (110). In virulent urinary organisms collected and curated by Anne-Catrin Uhlemann at Columbia University, we found that some clones utilized only heme transport, some only catecholate Ent transport, and others a combination of heme and ferric iron transport (**Figure 5**). This analysis is exciting because we recognize (*a*) that the heme nutritional pathway is pervasive in human UTI isolates; (*b*) nearly all isolates express Ent (subject to NGAL blockade) and, in fact, two clones express Ent as the single iron transport pathway; (*c*) one clone expresses heme capture and Ent alone; and (*d*) other clones express limited (UTI-89) or wide-ranging combinations (CFT073 and others).

TCS: two-component systems

Similar in purpose to the prevention of ferric iron theft (61), Iqbal Hamza and colleagues discovered a pathway to secure heme-iron, called Slc48a1: (*a*) Slc48a1 (111, 112) is localized to plasma and endosomal membranes (113, 114), including apical and basolateral surfaces of different cells (115); (*b*) Slc48a1 is modulated by heme levels (112) in a Bach1 (heme transcription factor) suppressible manner (116), and (*c*) overexpression of Slc48a1 in mammalian cells increases the import rate of heme analog, ZnMP (112, 114), while *Slc48a1* suppression by siRNA reduces uptake (114). *Slc48a1* is expressed in both the collecting ducts and the urothelium of the bladder.

In summary, for each attempt at iron capture by bacteria, urinary epithelia express competitive mechanisms. In the case of heme, it is reasonable to propose that urinary epithelia repurpose a metabolic role (clearing the urine of heme, hemoglobin, and iron) into an immune defense. The proposed mechanism capitalizes on low UpH, as Slc48a1 is a Heme/H^+ symporter (114).

Secondary Responses of Bacteria to Starvation: The Role of Two-Component Systems

Iron levels regulate many bacterial functions including resistance to defensins via two-component systems (TCS). TCS are ubiquitous and provide important mechanisms for bacteria to respond quickly to environmental signals relevant to the acquisition of nutrients, cell growth and division, the expression and regulation of virulence factors, and rapid defenses against environmental hazards, such as the host immune system. Moreover, TCS also play a role in cellular processes leading to antibiotic resistance in Gram-positive and -negative bacteria (117–119). This includes intrinsic tolerance of *E. coli* to polymyxins (120). TCS are notably absent from mammalian cells and thus potentially interesting novel targets for antimicrobial treatments.

In general, TCS consist of a membrane-embedded histidine kinase that acts as the sensor and signal receiver, whereas the response regulator is located in the cytoplasm. The rapid transmission of the signaling cascade is mediated by the sensor kinases that autophosphorylate at a conserved histidine residue, acting as a phosphodonor for subsequent phosphotransfer to and activation of a cognate response regulator. In some select cases, the histidine residue is also essential for response regulator dephosphorylation via a reverse-phosphotransfer reaction.

Supplemental Material >

E. coli, including UPEC, harbor over 60 TCS genes; many have not been evaluated in the context of UTI (**Supplemental Table 1**). The best characterized examples are the BarA-UvrY and QseBC systems.

The BarA-UvrY system regulates carbon storage and accessing carbon sources from the urine (121) and regulates virulence. Mutations in either of the two components decreased hemolysin and

LPS production and dampened proinflammatory cytokine and chemokine responses. The BarA-UvrY TCS also regulates the expression of noncoding regulatory CsrB and CsrC RNAs. CsrB and CsrC are in control of CsrA protein activity and have been shown to regulate key virulence functions in *E. coli* that are also relevant to UTIs, namely flagellar biosynthesis (122), biofilm formation, and carbon metabolism (123).

In contrast, the QseBC TCS regulates pili and membrane lipids and is sensitized by iron levels. Deletion of QseC (but not QseB or the entire operon) results in a major attenuation of virulence (124, 125) through decreased expression of motility genes, CUP systems (type 1 pili, curli fibers), and several metabolic pathways. Guckes et al. (120) showed that the QseB response regulator can interact with the PmrAB TCS. Specifically, PmrB (sensor kinase) was shown to constitutively phosphotransfer to QseB in the absence of the QseC sensor. In this setting, the constitutive activation results in the attenuation of virulence through the repression of QseC.

PmrAB and QseBC regulate resistance to the innate immune responses of the host. Recent evidence from UTI and many other types of models demonstrates that resistance is conferred by the interaction of two iron-dependent kinases in Enterobacterales with the property of mutual inhibition (PmrA–PmrB). These enzymes regulate the charge of cell surface LPS from anionic (defensin sensitive) to cationic (defensin resistant). PmrB responds to ferric iron and mediates alterations to the LPS layer of the outer membrane to protect the cell against cationic polypeptide stress. In the setting of acidosis and iron, the PmrA component directs the cell membrane to resist defensins (antimicrobial peptides) or its surrogate used in the lab, the antibiotic polymyxin. In UPEC, ferric iron activates both PmrA and QseB response regulators in a PmrB-dependent manner (120). Conversely, iron starvation is predicted to result in bacterial sensitivity to defensins. Consequently, PmrA and PmrB mutants should demonstrate reciprocal survival in iron-poor (such as iron chelation by siderophores and mammalian iron transport) and iron-rich settings, such as HMOX1 and Slc48A1 knockouts.

HCN: hyperpolarization-activated cation

TCC: T-type calcium channel

BIOPHYSICAL BARRIERS TO THE KIDNEYS

As can be seen from this brief review, many host defenses, including capture, starvation, and poisoning, are bacteriostatic and not bactericidal. Hence, mechanisms to expel the disabled UPEC are required.

Peristalsis

Peristaltic activity of the ureter is a barrier to ascending bacteria. Bacteria in turn can paralyze this mechanism. Research points to the hyperpolarization-activated cation (HCN) and T-type calcium channels (TCCs) as drivers of peristalsis (126). HCN channels mediate an inward cationic current that gradually depolarizes the cell and triggers activation of TCCs, which completes cellular depolarization (126) and regulates their frequency (127). Evidence points to HCN^{+} (128) interstitial cells of Cajal as the pacemakers. Alternatively, smooth muscle cells located in the human minor calyx and porcine calices (126) may serve as pacemakers, while the same activity locates in the ureter-pelvic junction in mice (127). The consensus from different articles points to HCN3 as the main HCN channel in mice, whereas HCN4 and HCN1 (128) are the main channels in human ureters.

The importance of ureteric peristalsis in preventing infection is suggested by depot-medroxyprogesterone acetate therapy. Data show that women taking depot-medroxyprogesterone acetate have higher rates of UTIs (129). Depot-medroxyprogesterone induces ureteric relaxation by promoting the expression of β2/3-adrenoreceptors (130, 131). It is thought that disruption of flow dynamics promotes urinary stasis and the proliferation of bacteria (129).

MDWP: monophasic Doppler waveform pattern

CIC: clean intermediate catheterization

SCI: spinal cord injury

To further evaluate the relationship between peristalsis and UTIs, it is worth studying the maturation of flow dynamics in infants. Newborns display immature monophasic Doppler waveform patterns (MDWPs) of ureteric jets at the vesicoureteral junction (132). The MDWPs resolve by four years of age when biphasic, triphasic, or polyphasic patterns of the ureteric jet are found (132). Persistence of MDWPs correlates with UTIs in young children (132). Children suffering from UTIs (without vesiculo-ureteral reflux) had an incidence of unilateral and bilateral MDWPs that was 1.7 and 2.5 times greater, respectively, than healthy controls (132). Hence, even simple alterations in ureteric peristalsis modify flow dynamics and encourage bacterial proliferation.

Additional data confirm the role of ureteral peristalsis in preventing kidney infection. Urinary pathogens appear to abrogate peristalsis, even causing hydronephrosis in humans (133, 134). Experiments conducted on cats and dogs demonstrated that chronic infection with uropathogens can abolish peristaltic activity of the ureters (135). Pathogenic strains reduced peristalsis by decreasing the Ca^{2+} transients (87) by various mechanisms including possible endogenous Ca^{2+} ionophores (133). Nonpathogenic bacteria, in contrast, did not cause uroplegia. In summary, peristalsis plays a vital role in urogenital defense, because its disruption or inappropriate functioning leads to UTI exacerbation. It also seems that by causing uroplegia, bacteria can initiate a cyclical relationship between dysfunction and infection. Careful documentation of the premorbid phenotype is required to help resolve whether ureteral dysfunction precedes and provides a risk for infection or whether infection causes ureteral dysfunction.

Urine Flow, Volume, and Obstruction

A reflexive response to UTI is to tell patients to drink plenty of fluids (e.g., water). Does a greater flow of urine provide a second type of barrier for ascending bacteria? Unexpectedly, the data are inconsistent (136). For example, a recent meta-analysis of recurrent UTIs (rUTIs) showed that an increase in oral fluids for 12 months produced an inadequate statistical difference with control patients ($p = 0.06$). In contrast, studies that measured increased fluid consumption for $\leq$6 months demonstrated a strong positive effect (OR 0.13, 95% CI, 0.07–0.25; $p < 0.001$) (137). In premenopausal women who suffer from recurrent cystitis and consumed <1.5 L of water per day, increasing water intake significantly decreased rUTIs, with a mean reduction of 1.5 cases of recurrent cystitis (95% CI, 1.2–1.8; $p < 0.001$) (138). In nursing home residents, increased consumption of fluid by 200–400 mL daily decreased UTIs from 51 to 37, albeit statistically insignificant ($p = 0.625$) (139).

One would think that if flow were vital for combatting UTIs (140, 141), then disruption of urine flow by obstructive uropathy (142–144) should led to higher rates of UTI. The observation is not so simple, however, because obstruction may damage the antimicrobial activities of the collecting duct (see above). In addition, the tools available to enhance flow are confounded. For example, restoring flow by clean intermediate catheterization (CIC) in patients with spinal cord injury (SCI) should enable proper clearance of bacteria. Yet, CIC is associated with recurrent or continuous bacteriuria (145). The effect may be due to catheter-mediated damage of urothelium (146) or the introduction of bacteria by the foreign body. In fact, a study of 369 SCI inpatients showed that the use of any method of catheterization, as opposed to spontaneous voiding, was the primary determinant of elevated UTI risk (147). Flushing the catheters also enhanced risk (148, 149). Hence, damage inflicted by catheters confounded the flow data.

Nonetheless, chronic bladder dysfunction in animal models is also associated with UTIs (150). SCI-induced voiding dysfunction in rats resulted in pronounced inflammatory responses to subacute infections and prolonged the UTI (151). The proximate reason for these findings may have more to do with changes in the urothelium than flow disturbances, however, as post-void residuals did not predict infection susceptibility or severity (151).

A second line of reasoning attempting to illuminate the contribution of flow comes from the evaluation of obstructive uropathy due to stone disease. Here again, there are a number of issues to tackle before establishing causality. The central premise is that urine concentration results in supersaturation with either calcium, oxaloacetate, phosphate, and other inorganic compounds (152), resulting in stone disease that obstructs flow and creates higher bacterial loads (153). This premise leads to the well-known therapy of increasing oral water intake to diminish supersaturation and reduce urinary obstruction and urinary infection. However, the literature suggests a more nuanced pathogenesis that ties together urine concentration, stone formation, and UTI. First, calculi formation was only modestly decreased by interventions that diminished supersaturability (154–156). Second, subjects suffering from nephrolithiasis had overlapping urinalysis with normal patients (157), implicating a missing component that triggered stone disease. Synergy between inorganic components and urinary bacteria may be this missing component. At the initiation of the pathway, neither calcium oxalate nor urinary bacteria themselves can catalyze stone formation (158), but when the host is at saturation, uropathogenic bacteria trigger an innate immune reaction, which forms the nidus for crystallization (158). Hence, it seems that infection triggers the obstruction, rather than the obstruction initiating the infection (159).

NCC: thiazide-sensitive Na^+-Cl^- symporter

In summary, the data suggest that flow is a biophysical component of innate immune defense, and if not to inhibit initiation of infection then probably to suppress its amplification. Yet, the precise interaction of flow and infection is likely mediated by complex cellular events, beyond the biophysical nature of flow. It is possible that variability between studies hinges on competing outcomes secondary to an increased flow of dilute urine. Oral rehydration is based on the notion that increased flow enhances bacterial expulsion, but by regulating vasopressin and suppressing medullary hypertonicity, chronic rehydration conceivably can suppress immune regulation. A parallel consideration applies to obstructive uropathy, which is also associated with vasopressin resistance (160). The details of this finely balanced system are discussed below.

RENAL PHYSIOLOGY CALLS IN THE IMMUNE SYSTEM

Hyperosmolarity

It is remarkable that bacterial infection can take place in the hostile chemical environment of the renal medulla. Some of this chemistry is central to the homeostatic functions of the kidney (e.g., Na gradient, pH gradient) but repurposed for bacteriostatic responses.

The kidney regulates water balance in part by removing NaCl from lumen and creating a hyperosmotic interstitium in response to vasopressin receptor 2 (V2R) in human TALH and distal convoluted tubules (161). Activation of V2R leads to the activation of NKCC2 and the thiazide-sensitive Na^+-Cl^- symporter (NCC) by phosphorylation (162). These transporters play a crucial role in the maintenance of the osmotic gradient.

The transport of Na and the creation of an osmotic gradient play surprising roles in immune defense. Medullary Na signals nuclear factor of activated T cells 5 (NFAT5) in the collecting epithelia, which in turn express CCL2, a cytokine that generates $CD14^+$ mononuclear cells that will go on to phagocytize UPEC. The finding that Na concentration plays a role in immune defense has extensive support. (*a*) Human kidney epithelia HK2 and HEK293 T exposed to concentrated solutions of Na^+ (up to 250 mM) upregulated NFAT5 and stimulated the downstream genes *CX3CL1* and *CCL2* (163). Hyperosmotic sensing is mediated by protein kinase A–anchoring protein 13 (Brx), a guanine nucleotide exchange factor that functions as a positive regulator of small G proteins (164). Brx in turn activates the small G proteins Cdc42 and Rac1, which mediate Brx interactions with p38 MAPK-specific scaffold protein c-Jun N-terminal kinase (JNK)–interacting

protein 4 (JIP4) (164). p38 MAPK activation subsequently activates NFAT5 transcription. Hence, Na hyperosmolarity translates to NFAT5 expression via p38 MAPK. In a kidney cell line NRK52, hypersalinity consistently induced CCL2 through p38 MAPK, ERK. (*b*) Conversely, the suppression of the Na^+ gradient in the human due to washout induced by diabetes insipidus reduced medullary expression of NFAT5 and its dependent gene product chemokines such as CX3CL1 and CCL2 and reduced $CD14^+$ cell migration to the renal medulla. (*c*) Induction of diabetes insipidus by demeclocycline or tolvaptan in rats, which reduced urine concentration capacity, resulted in the loss of expression of NFAT5-dependent genes and CCL2 and superinfection with UPEC (163). In fact, mice whose V2Rs were pharmacologically blocked and whose medullary Na^+ gradient was disrupted had a higher incidence of bacteremia and death (163). Similar results were observed in humans, where there was a dose-dependent correlation of treatment with tolvaptan, a V2R antagonist, and the incidence of UTIs (165). (*d*) Suppression of NKCC2 and NCC transporters by diuretics may increase the incidence of UTIs. Although the literature on the effects of diuretics on urinary infection is scant, some articles do report a correlation of the use of loop and thiazide diuretics with lower urinary tract symptoms. In addition, a 5-year longitudinal study following up on renal transplant patients found an association between diuretics and higher rates of UTIs (166). Patients who received higher doses of loop diuretics had a diminished ratio of M1/M2 macrophages in the medullary region of their kidneys (166), likely due to reduced medullary Na^+ gradients resulting from diuretic therapy. A diminished population of M1 macrophages (167) may explain the higher incidence of kidney infection. (*e*) A number of clinical observations can now be interpreted as attempts to maximize the Na gradient in the setting of UTI. For example, activation of intrarenal renin-angiotensin-aldosterone system activity (168) following pyelonephritis in children results in a decrease in urinary Na^+ (uNa), a decrease in urinary Na^+/K^+ ratio (uNa/K), and decreased fractional excretion of Na^+, conceivably contributing to the medullary Na gradient by activating transport into the medulla. Indeed, this system may drive the hypothesis that some patients suffering from pyelonephritis develop hypertension and are unable to excrete Na^+ appropriately (169, 170).

Medullary hypersalinity recruits $CD14^+$ monocyte-derived mononuclear phagocytes (MNPs) to the kidney medulla via CCL2. Recruitment of human $CD14^+$ cells (163) is critical because these cells are more efficient than cortical $CD14^-$ MNPs at phagocytizing UPEC and secreting factors IL-6, IL-8, and tumor necrosis factor alpha (TNF-α). In fact, the Na gradient is directly responsible for priming the responses of the $CD14^+$ MNP, including the migration toward tissues expressing high levels of the chemokines CX3CL1 and CCL2 and UPEC phagocytosis in both human and murine monocytes. In addition, factors secreted by $CD14^+$ cells secondarily increase neutrophil response to UPEC, which makes the recruitment of medullary $CD14^+$ cells crucial for mounting a strong response. Hence, the Na^+ gradient initiates epithelia cell signaling to monocytes to guide their recruitment.

The Na gradient also has an effect in T cell maturation. Augmenting extracellular NaCl in the presence of T helper (Th)17-inducing cytokines shifts naive human $CD4^+$ T cells toward the Th17 phenotype in both in vitro and in vivo experiments (171). These immune cells are involved in host defense against different types of microbes. Under these hyperosmolar conditions, they secreted not only IL-17 but also IL-2, TNF-α, IL-9, GM-CSF, TBX21, and CCR6 (171).

In summary, the medullary Na gradient profoundly enhances immune responses in the kidney. This optimized immune response is strategically positioned because an ascending UPEC infection will first encounter the medullary hyperosmotic region of the kidney. High medullary Na^+ concentration states, such as during dehydration, might optimize the system to suppress bacterial growth.

Fluid Therapy for Setting a Medullary Na Gradient

FSS: flow-shear stress

The physiologic data indicate that the Na gradient is repurposed to guide immune responses. It is apparent from the prior argument that volume depletion should stimulate the Na gradient across the inner medulla via stimulation of aldosterone and vasopressin. Volume depletion would enhance the Na gradient and provide compensatory protection from UTI when flow rates are diminished. In this case, chronic attempts at volume expansion and high flow rates (as we saw with diabetes insipidus and diuretics or even possibly in some of the clinical studies listed above) might diminish the Na gradient and hence are counterproductive to immune defense. However, one can also imagine that volume depletion limits delivery of Na^+ beyond the cortex so that limited volume expansion may acutely protect medullary gradients by Na delivery.

Volume expansion can regulate other pathways that impact the medullary Na^+ gradient. In proximal tubular epithelial cells and in collecting ducts, the main pathway activated by flow-shear stress (FSS) is transforming growth factor-β (TGF-β)/ALK5 receptor (172). TGF-β1 is relevant in the context of UTIs because it can downregulate the immune system response (173) and enhance prostaglandin endoperoxidase synthase2, the *COX-2* gene, which regulates the Na gradient by promoting natriuresis and inhibiting water reabsorption in the inner medullary collecting duct. Indeed, in rats, *COX-2* is activated by FSS-dependent neutral-sphingomyelinase (174), which induces the production of prostaglandin E_2 (PGE_2). Subsequently, under high FSS, PGE_2 production blunts Na^+ reabsorption in the TALH and in the cortical collecting duct cells (175), potentially contributing to the wash out of the interstitial Na^+ gradient in the setting of high flow. Conversely, *COX-2* inhibition of the renal medulla leads to Na^+ retention (176).

FSS also acts by simulating a second pathway that reduces Na^+ retention. The nonselective cation Piezo1 mechanoreceptors are activated through stretch and flow mechanisms (177, 178). Piezo1 has been documented as responding to direct force on the lipid bilayer of the cell membrane (179). Piezo mechanoreceptors are concentrated on the basolateral side of kidney epithelia, implying that the receptors' primary responsibility is to detect changes in tension within the urinary system (180). They are highly expressed in the inner medullary collecting duct of the kidney (180, 181), presumably measuring medullary mechanical forces.

Piezo1 induces an increase in intracellular Ca^{+2} concentration (177), which perhaps via PLA2 (182) results in the production of PGE_2, creating a natriuretic effect. A recent study on murine collecting ducts demonstrated that Piezo1 influences urine dilution following dehydration (180) by the following sequence: Piezo1 induces Ca^{+2} influx, decreasing the production of intracellular cAMP, resulting in the retrieval of aquaporin 2 from the plasma membrane. Therefore, it is proposed that Piezo1 plays the regulatory role in preventing excessive changes in the medullary Na^+ gradient upon acute rehydration by quickly withdrawing the aquaporin 2 channels, while simultaneously increasing natriuresis. This concept would posit flow as an entity that maintains the medullary Na^+ gradient via Piezo channels and via the effect of prostaglandins.

In summary, an increase in water intake will suppress vasopressin release and hence vasopressin-dependent Na reabsorption in the distal nephron. In addition, given the residual permeability to water, even when vasopressin is suppressed, high flow can potentially diminish the medullary Na^+ gradient, which is an important signal for an optimal immune response. These results might explain the variability in rehydration studies and suggest that careful urinary metrics referable to medullary function could optimize the dose of directed fluid therapy in attempts to suppress UTI.

CONCLUSIONS

The invasion of the urinary tract by bacteria is met with a variety of defenses that limit their growth (bacteriostatic) or cause their death (bactericidal). Bacteriostatic responses include

physical capture by uromodulin; suppression of epithelial attachment and bacterial growth by acidification; starvation by the capture of iron (e.g., lactoferrin), the capture and metabolism of heme [e.g., HRG1 (Slc48a1)], and the capture of bacterial siderophores [NGAL (siderocalin)]; poisoning by CO gas; expulsion by urinary flow and ureteral peristalsis; and Na-dependent signaling to bactericidal phagocytes. Each bacteriostatic mechanism shortens the duration of the infection and reduces colony counts.

Yet, linkage and coordination between these defenses have not been unraveled. Compelling examples include the expression of innate immune defense molecules by the kidney in models of cystitis as well as the use of the Na gradient to summon phagocytes. The induction of IL-8 by apo-Ent and NGAL (183, 184) is another example of coordination that should be examined in the urinary tract.

A second critical area for analysis is revisiting the causal sequence. A fascinating example includes the observation that flow disturbances presage infection. Yet there is evidence that UPEC suppress ureteral peristalsis and cause flow disturbances. Obstruction by stone disease is associated with infection, but there is evidence that infection is a nidus for crystallization. Water hydration should reduce the bacterial burden by increasing flow rate, but an increase in flow has been associated with infection.

Unraveling these mechanisms has clinical consequences. These include the use of iron supplements and iron chelation because excess iron stimulates bacterial growth and iron sequestration is protective (e.g., NGAL, lactoferrin, anemia of chronic disease). Additionally, the TCS, which determines sensitivity to defensins, is iron sensitive. Moreover, antibiotic therapy may play a role in flow disturbances, as infection may initiate ureteral paralysis and seed stone formation. Finally, even a simple therapy, hydration, requires reconsidering the context of bacteriostatic mechanisms of the urinary tract.

DISCLOSURE STATEMENT

The authors are not aware of any affiliations, memberships, funding, or financial holdings that might be perceived as affecting the objectivity of this review.

ACKNOWLEDGMENTS

The authors would like to acknowledge the dedicated work of scientists and physicians studying "Benign Urology," a diverse set of diseases that afflict nearly all humans. The authors acknowledge the many data contributions of Roland Strong (Fred Hutchinson Cancer Research Center), and Katherine Xu, Abraham Levitman, and Tian Shen (Columbia University). J.B. and A.-C.U. are supported by the O'Brien Center for Benign Urology at Columbia University (U54DK104309). J.B. is also supported by the NIH–NIDDK's Kidney Precision Medicine Project (4UH3DK114926).

LITERATURE CITED

1. Flores-Mireles AL, Walker JN, Caparon M, Hultgren SJ. 2015. Urinary tract infections: epidemiology, mechanisms of infection and treatment options. *Nat. Rev. Microbiol.* 13(5):269–84
2. Foxman B. 2014. Urinary tract infection syndromes. Occurrence, recurrence, bacteriology, risk factors, and disease burden. *Infect. Dis. Clin. North Am.* 28(1):1–13
3. McLellan LK, Hunstad DA. 2016. Urinary tract infection: pathogenesis and outlook *Trends Mol. Med.* 22(11):946–57
4. Klein RD, Hultgren SJ. 2020. Urinary tract infections: microbial pathogenesis, host-pathogen interactions and new treatment strategies *Nat. Rev. Microbiol.* 18(4):211–26

5. Johnson JR, Russo TA. 2018. Acute pyelonephritis in adults. *N. Engl. J. Med.* 378(1):48–59
6. Piccoli GB, Consiglio V, Colla L, Mesiano P, Magnano A, et al. 2006. Antibiotic treatment for acute "uncomplicated" or "primary" pyelonephritis: a systematic, "semantic revision." *Int. J. Antimicrob. Agents* 28(Suppl. 1):49–63
7. Forster CS, Jackson E, Ma Q, Bennett M, Shah SS, Goldstein SL. 2018. Predictive ability of NGAL in identifying urinary tract infection in children with neurogenic bladders. *Pediatr. Nephrol.* 33(8):1365–74
8. Paragas N, Kulkarni R, Werth M, Schmidt-Ott KM, Forster C, et al. 2014. α-Intercalated cells defend the urinary system from bacterial infection. *J. Clin. Investig.* 124(7):2963–76
9. Hannan TJ, Mysorekar IU, Hung CS, Isaacson-Schmid ML, Hultgren SJ. 2010. Early severe inflammatory responses to uropathogenic *E. coli* predispose to chronic and recurrent urinary tract infection. *PLOS Pathog.* 6(8):29–30
10. Ingersoll MA, Kline KA, Nielsen HV, Hultgren SJ. 2008. G-CSF induction early in uropathogenic *Escherichia coli* infection of the urinary tract modulates host immunity. *Cell. Microbiol.* 10(12):2568–78
11. Sundén F, Butler D, Wullt B. 2017. Triggered urine interleukin-6 correlates to severity of symptoms in nonfebrile lower urinary tract infections. *J. Urol.* 198(1):107–15
12. Park J, Shrestha R, Qiu C, Kondo A, Huang S, et al. 2018. Single-cell transcriptomics of the mouse kidney reveals potential cellular targets of kidney disease. *Science* 360(6390):758–63
13. Werth M, Schmidt-Ott KM, Leete T, Qiu A, Hinze C, et al. 2017. Transcription factor *TFCP2l1* patterns cells in the mouse kidney collecting ducts. *eLife* 6:e24265
14. Chassin C, Goujon J-M, Darche S, du Merle L, Bens M, et al. 2006. Renal collecting duct epithelial cells react to pyelonephritis-associated *Escherichia coli* by activating distinct TLR4-dependent and -independent inflammatory pathways. *J. Immunol.* 177(7):4773–84
15. Becknell B, Schwaderer A, Hains DS, Spencer JD. 2015. Amplifying renal immunity: the role of antimicrobial peptides in pyelonephritis. *Nat. Rev. Nephrol.* 11(11):642–55
16. McLellan LK, McAllaster MR, Kim AS, Tóthová Ľ, Olson PD, et al. 2021. A host receptor enables type 1 pilus-mediated pathogenesis of *Escherichia coli* pyelonephritis. *PLOS Pathog.* 17(1):e1009314
17. Chassin C, Vimont S, Cluzeaud F, Bens M, Goujon JM, et al. 2008. TLR4 facilitates translocation of bacteria across renal collecting duct cells. *J. Am. Soc. Nephrol.* 19(12):2364–74
18. Wang C, Li Q, Lv J, Sun X, Cao Y, et al. 2020. Alpha-hemolysin of uropathogenic *Escherichia coli* induces GM-CSF-mediated acute kidney injury. *Mucosal Immunol.* 13(1):22–33
19. Uhlén P, Laestadius Å, Jahnukainen T, Söderblum T, Bäckhed F, et al. 2000. α-Haemolysin of uropathogenic *E. coli* induces Ca^{2+} oscillations in renal epithelial cells. *Nature* 405(6787):694–97
20. Johnsen N, Hamilton ADM, Greve AS, Christensen MG, Therkildsen JR, et al. 2019. α-Haemolysin production, as a single factor, causes fulminant sepsis in a model of *Escherichia coli*-induced bacteraemia. *Cell. Microbiol.* 21(6):e13017
21. Hinze C, Karaiskos N, Boltengagen A, Walentin K, Redo K, et al. 2021. Kidney single-cell transcriptomes predict spatial corticomedullary gene expression and tissue osmolality gradients. *J. Am. Soc. Nephrol.* 32(2):291–306
22. Miyazaki T, Gharib SA, Hsu YWA, Xu K, Khodakivskyi P, et al. 2019. Cell-specific image-guided transcriptomics identifies complex injuries caused by ischemic acute kidney injury in mice. *Commun. Biol.* 2(1):326
23. Parish A, Holliday K. 2012. Long-term care acquired urinary tract infections' antibiotic resistance patterns and empiric therapy: a pilot study. *Geriatr. Nurs.* 33(6):473–78
24. Palou J, Angulo JC, Ramón de Fata F, García-Tello A, González-Enguita C, et al. 2013. Randomized comparative study for the assessment of a new therapeutic schedule of fosfomycin trometamol in postmenopausal women with uncomplicated lower urinary tract infection. *Actas Urol. Esp.* 37(3):147–55
25. Hof H. 2017. Candiduria! What now? Therapy of urinary tract infections with *Candida*. *Urologe* 56(2):172–79
26. Spaulding CN, Hultgren SJ. 2016. Adhesive pili in UTI pathogenesis and drug development. *Pathogens* 5(1):30
27. Sarkar S, Hutton ML, Vagenas D, Ruter R, Schüller S, et al. 2018. Intestinal colonization traits of pandemic multidrug-resistant *Escherichia coli* ST131. *J. Infect. Dis.* 218(6):979–90

28. Biggel M, Xavier BB, Johnson JR, Nielsen KL, Frimodt-Møller N, et al. 2020. Horizontally acquired *papGII*-containing pathogenicity islands underlie the emergence of invasive uropathogenic *Escherichia coli* lineages. *Nat. Commun.* 11(1):5968
29. Poole J, Day CJ, Von Itzstein M, Paton JC, Jennings MP. 2018. Glycointeractions in bacterial pathogenesis *Nat. Rev. Microbiol.* 16(7):440–52
30. Pak J, Pu Y, Zhang ZT, Hasty DL, Wu XR. 2001. Tamm-Horsfall protein binds to type 1 fimbriated *Escherichia coli* and prevents *E. coli* from binding to uroplakin Ia and Ib receptors. *J. Biol. Chem.* 276(13):9924–30
31. Garimella PS, Bartz TM, Ix JH, Chonchol M, Shlipak MG, et al. 2017. Urinary uromodulin and risk of urinary tract infections: the cardiovascular health study. *Am. J. Kidney Dis.* 69(6):744–51
32. Bates JM, Raffi HM, Prasadan K, Mascarenhas R, Laszik Z, et al. 2004. Tamm-Horsfall protein knockout mice are more prone to urinary tract infection. *Kidney Int.* 65(3):791–97
33. Weiss GL, Stanisich JJ, Sauer MM, Lin CW, Eras J, et al. 2020. Architecture and function of human uromodulin filaments in urinary tract infections. *Science* 369(6506):1005–10
34. Brunati M, Perucca S, Han L, Cattaneo A, Consolato F, et al. 2015. The serine protease hepsin mediates urinary secretion and polymerisation of Zona Pellucida domain protein uromodulin. *eLife* 4:e08887
35. Shohl AT, Janney JH. 1917. The growth of Bacillus coli in urine at varying hydrogen ion concentrations. *J. Urol.* 1(2):211–12
36. de Souza BSV, Silva KCS, Parente AFA, Borges CL, Paccez JD, et al. 2019. The influence of pH on *Staphylococcus saprophyticus* iron metabolism and the production of siderophores. *Microbes Infect.* 21(10):456–63
37. Carpenter MA, Hoberman A, Mattoo TK, Mathews R, Keren R, et al. 2013. The RIVUR trial: profile and baseline clinical associations of children with vesicoureteral reflux. *Pediatrics* 132(1):e34–45
38. Hoberman A, Charron M, Hickey RW, Baskin M, Kearney DH, Wald ER. 2003. Imaging studies after a first febrile urinary tract infection in young children. *N. Engl. J. Med.* 348(3):195–202
39. Guizar JM, Kornhauser C, Malacara JM, Sanchez G, Zamora J. 1996. Renal tubular acidosis in children with vesicoureteral reflux. *J. Urol.* 156(1):193–95
40. Chandar J, Abitbol C, Novak M, Zilleruelo G, Strauss J. 1999. Abnormal urinary acidification in infants with hydronephrosis. *Pediatr. Nephrol.* 13(4):315–18
41. Hiatt MJ, Ivanova L, Toran N, Tarantal AF, Matsell DG. 2010. Remodeling of the fetal collecting duct epithelium. *Am. J. Pathol.* 176(2):630–37
42. Hiatt MJ, Ivanova L, Trnka P, Solomon M, Matsell DG. 2013. Urinary tract obstruction in the mouse: the kinetics of distal nephron injury. *Lab. Investig.* 93(9):1012–23
43. Wang G, Li C, Kim SW, Ring T, Wen J, et al. 2008. Ureter obstruction alters expression of renal acid-base transport proteins in rat kidney. *Am. J. Physiol. Renal Physiol.* 295(2):F497–506
44. Wang G, Ring T, Li C, Kim SW, Wen J, et al. 2009. Unilateral ureteral obstruction alters expression of acid-base transporters in rat kidney. *J. Urol.* 182(6):2964–73
45. Kanemitsu H, Sasaki S, Akiba T, Marumo F. 1990. Ureteral obstruction decreases ATP dependent H^+-pump activity of rabbit renal outer medulla. *Tohoku J. Exp. Med.* 160(3):223–29
46. Purcell H, Bastani B, Harris KPG, Hemken P, Klahr S, Gluck S. 1991. Cellular distribution of H^+-ATPase following acute unilateral ureteral obstruction in rats. *Am. J. Physiol. Ren. Fluid Electrolyte Physiol.* 261(3):F365–76
47. Han JS, Kim GH, Kim J, Jeon US, Joo KW, et al. 2002. Secretory-defect distal renal tubular acidosis is associated with transporter defect in H^+-ATpase and anion exchanger-1. *J. Am. Soc. Nephrol.* 13(6):1425–32
48. Schwan WR, Lee JL, Lenard FA, Matthews BT, Beck MT. 2002. Osmolarity and pH growth conditions regulate *fim* gene transcription and type 1 pilus expression in uropathogenic *Escherichia coli*. *Infect. Immun.* 70(3):1391–402
49. Peng H, Purkerson JM, Freeman RS, Schwaderer AL, Schwartz GJ. 2020. Acidosis induces antimicrobial peptide expression and resistance to uropathogenic *E. coli* infection in kidney collecting duct cells via HIF-1α. *Am. J. Physiol. Ren. Physiol.* 312(2):F468–74
50. Lai HC, Chang SN, Lin HC, Hsu YL, Wei HM, et al. 2019. Association between urine pH and common uropathogens in children with urinary tract infections. *J. Microbiol. Immunol. Infect.* 54(2):290–98

51. Chipperfield JR, Ratledge C. 2000. Salicylic acid is not a bacterial siderophore: a theoretical study. *BioMetals* 13(2):165–68
52. Bao G, Clifton M, Hoette TM, Mori K, Deng SX, et al. 2010. Iron traffics in circulation bound to a siderocalin (Ngal)-catechol complex. *Nat. Chem. Biol.* 6(8):602–9
53. Skaar EP. 2010. The battle for iron between bacterial pathogens and their vertebrate hosts. *PLOS Pathog.* 6(8):e1000949
54. Brzuszkiewicz E, Brüggemann H, Liesegang H, Emmerth M, Ölschläger T, et al. 2006. How to become a uropathogen: comparative genomic analysis of extraintestinal pathogenic *Escherichia coli* strains. *PNAS* 103(34):12879–84
55. Thulasiraman P, Newton SMC, Xu J, Raymond KN, Mai C, et al. 1998. Selectivity of ferric enterobactin binding and cooperativity of transport in gram-negative bacteria. *J. Bacteriol.* 180(24):6689–96
56. Shields-Cutler RR, Crowley JR, Miller CD, Stapleton AE, Cui W, Henderson JP. 2016. Human metabolome-derived cofactors are required for the antibacterial activity of siderocalin in urine. *J. Biol. Chem.* 291(50):25901–10
57. Hagan EC, Lloyd AL, Rasko DA, Faerber GJ, Mobley HLT. 2010. *Escherichia coli* global gene expression in urine from women with urinary tract infection. *PLOS Pathog.* 6(11):e1001187
58. Russo TA, McFadden CD, Carlino-MacDonald UB, Beanan JM, Olson R, Wilding GE. 2003. The siderophore receptor IroN of extraintestinal pathogenic *Escherichia coli* is a potential vaccine candidate. *Infect. Immun.* 71(12):7164–69
59. Goetz DH, Holmes MA, Borregaard N, Bluhm ME, Raymond KN, Strong RK. 2002. The neutrophil lipocalin NGAL is a bacteriostatic agent that interferes with siderophore-mediated iron acquisition. *Mol. Cell* 10(5):1033–43
60. Barasch J, Hollmen M, Deng R, Hod EA, Rupert PB, et al. 2016. Disposal of iron by a mutant form of lipocalin 2. *Nat. Commun.* 7:12973
61. Barasch J, Mori K. 2004. Cell biology: iron thievery. *Nature* 432(7019):811–13
62. Allred BE, Correnti C, Clifton MC, Strong RK, Raymond KN. 2013. Siderocalin outwits the coordination chemistry of vibriobactin, a siderophore of *Vibrio cholerae*. *ACS Chem. Biol.* 8(9):1882–87
63. Bao GH, Barasch J, Xu J, Wang W, Hu FL, Deng SX. 2015. Purification and structural characterization of "simple catechol", the NGAL-siderocalin siderophore in human urine. *RSC Adv.* 5(36):28527–35
64. Spencer JD, Schwaderer AL, Wang H, Bartz J, Kline J, et al. 2013. Ribonuclease 7, an antimicrobial peptide upregulated during infection, contributes to microbial defense of the human urinary tract. *Kidney Int.* 83(4):615–25
65. Bagshaw SM, Bennett M, Haase M, Haase-Fielitz A, Egi M, et al. 2010. Plasma and urine neutrophil gelatinase-associated lipocalin in septic versus non-septic acute kidney injury in critical illness. *Intensive Care Med.* 36(3):452–61
66. Wheeler DS, Devarajan P, Ma Q, Harmon K, Monaco M, et al. 2008. Serum neutrophil gelatinase-associated lipocalin (NGAL) as a marker of acute kidney injury in critically ill children with septic shock. *Crit. Care Med.* 36(4):1297–303
67. Parravicini E, Nemerofsky SL, Michelson KA, Huynh TK, Sise ME, et al. 2010. Urinary neutrophil gelatinase-associated lipocalin is a promising biomarker for late onset culture-positive sepsis in very low birth weight infants. *Pediatr. Res.* 67(6):636–40
68. Paragas N, Qiu A, Zhang Q, Samstein B, Deng SX, et al. 2011. The Ngal reporter mouse detects the response of the kidney to injury in real time. *Nat. Med.* 17(2):216–22
69. Nickolas TL, Forster CS, Sise ME, Barasch N, Sola-Del Valle D, et al. 2012. NGAL (Lcn2) monomer is associated with tubulointerstitial damage in chronic kidney disease. *Kidney Int.* 82(6):718–22
70. Kanda J, Mori K, Kawabata H, Kuwabara T, Mori KP, et al. 2015. An AKI biomarker lipocalin 2 in the blood derives from the kidney in renal injury but from neutrophils in normal and infected conditions. *Clin. Exp. Nephrol.* 19(1):99–106
71. Fischbach MA, Lin H, Zhou L, Yu Y, Abergel RJ, et al. 2006. The pathogen-associated *iroA* gene cluster mediates bacterial evasion of lipocalin 2. *PNAS* 103(44):16502–7
72. Carbonetti NH, Boonchai S, Parry SH, Väisänen-Rhen V, Korhonen TK, Williams PH. 1986. Aerobactin-mediated iron uptake by *Escherichia coli* isolates from human extraintestinal infections. *Infect. Immun.* 51(3):966–68

73. Crosa JH. 1989. Genetics and molecular biology of siderophore-mediated iron transport in bacteria. *Microbiol. Rev.* 53(4):517–30
74. Watts RE, Totsika M, Challinor VL, Mabbett AN, Ulett GC, et al. 2012. Contribution of siderophore systems to growth and urinary tract colonization of asymptomatic bacteriuria *Escherichia coli*. *Infect. Immun.* 80(1):333–44
75. Russo TA, Olson R, MacDonald U, Beanan J, Davidson BA. 2015. Aerobactin, but not yersiniabactin, salmochelin, or enterobactin, enables the growth/survival of hypervirulent (hypermucoviscous) *Klebsiella pneumoniae* ex vivo and in vivo. *Infect. Immun.* 83(8):3325–33
76. Mulvey MA, Schilling JD, Hultgren SJ. 2001. Establishment of a persistent *Escherichia coli* reservoir during the acute phase of a bladder infection. *Infect. Immun.* 69(7):4572–79
77. Opal SM, Cross AS, Gemski P, Lyhte LW. 1990. Aerobactin and α-hemolysin as virulence determinants in *Escherichia coli* isolated from human blood, urine, and stool. *J. Infect. Dis.* 161(4):794–96
78. Law D, Kelly J. 1995. Use of heme and hemoglobin by *Escherichia coli* O157 and other Shiga-like-toxin-producing *E. coli* serogroups. *Infect. Immun.* 63(2):700–2
79. Ristow LC, Welch RA. 2016. Hemolysin of uropathogenic *Escherichia coli*: a cloak or a dagger? *Biochim. Biophys. Acta* 1858(3):538–45
80. Mariani AJ, Mariani MC, Macchioni C, Stams UK, Hariharan A, Moriera A. 1989. The significance of adult hematuria: 1,000 hematuria evaluations including a risk-benefit and cost-effectiveness analysis. *J. Urol.* 141(2):350–55
81. Addis T. 1926. The number of formed elements in the urinary sediment of normal individuals. *J. Clin. Investig.* 2(5):409–15
82. Goldring W. 1931. Studies of the kidney in acute infection. *J. Clin. Investig.* 10(2):355–67
83. Andrews SC, Robinson AK, Rodríguez-Quiñones F. 2003. Bacterial iron homeostasis. *FEMS Microbiol. Rev.* 27(2–3):215–37
84. Chung A, Arianayagam M, Rashid P. 2010. Bacterial cystitis in women. *Aust. Fam. Phys.* 39(5):295–98
85. Tolosano E, Fagoonee S, Morello N, Vinchi F, Fiorito V. 2010. Heme scavenging and the other facets of hemopexin. *Antioxid. Redox Signal.* 12(2):305–20
86. Otto BR, Verweij-Van Vught AMJJ, Maclaren DM. 1992. Transferrins and heme-compounds as iron sources for pathogenic bacteria. *Crit. Rev. Microbiol.* 18(3):217–33
87. Ascenzi P, Bocedi A, Visca P, Altruda F, Tolosano E, et al. 2005. Hemoglobin and heme scavenging. *IUBMB Life* 57(11):749–59
88. Cope LD, Thomas SE, Hrkal Z, Hansen EJ. 1998. Binding of heme-hemopexin complexes by soluble HxuA protein allows utilization of this complexed heme by *Haemophilus influenzae*. *Infect. Immun.* 66(9):4511–16
89. Choby JE, Skaar EP. 2016. Heme synthesis and acquisition in bacterial pathogens. *J. Mol. Biol.* 428(17):3408–28
90. Hagan EC, Mobley HLT. 2009. Haem acquisition is facilitated by a novel receptor Hma and required by uropathogenic *Escherichia coli* for kidney infection. *Mol. Microbiol.* 71(1):79–91
91. Torres AG, Payne SM. 1997. Haem iron-transport system in enterohaemorrhagic *Escherichia coli* O157:H7. *Mol. Microbiol.* 23(4):825–33
92. Garcia EC, Brumbaugh AR, Mobley HLT. 2011. Redundancy and specificity of *Escherichia coli* iron acquisition systems during urinary tract infection. *Infect. Immun.* 79(3):1225–35
93. Subashchandrabose S, Smith SN, Spurbeck RR, Kole MM, Mobley HLT. 2013. Genome-wide detection of fitness genes in uropathogenic *Escherichia coli* during systemic infection. *PLOS Pathog.* 9(12):e1003788
94. Stojiljkovic I, Hantke K. 1994. Transport of haemin across the cytoplasmic membrane through a haemin-specific periplasmic binding-protein-dependent transport system in *Yersinia enterocolitica*. *Mol. Microbiol.* 13(4):719–32
95. Stojiljkovic I, Hantke K. 1992. Hemin uptake system of *Yersinia enterocolitica*: similarities with other TonB-dependent systems in Gram-negative bacteria. *EMBO J.* 11(12):4359–67
96. Zhu W, Hunt DJ, Richardson AR, Stojiljkovic I. 2000. Use of heme compounds as iron sources by pathogenic Neisseriae requires the product of the *hemO* gene. *J. Bacteriol.* 182(2):439–47

97. Schmitt MP. 1997. Utilization of host iron sources by *Corynebacterium diphtheriae*: identification of a gene whose product is homologous to eukaryotic heme oxygenases and is required for acquisition of iron from heme and hemoglobin. *J. Bacteriol.* 179(3):838–45
98. Cornejo J, Willows RD, Beale SI. 1998. Phytobilin biosynthesis: cloning and expression of a gene encoding soluble ferredoxin-dependent heme oxygenase from *Synechocystis* sp. PCC 6803. *Plant J.* 15(1):99–107
99. Friedman J, Lad L, Li H, Wilks A, Poulos TL. 2004. Structural basis for novel δ-regioselective heme oxygenation in the opportunistic pathogen *Pseudomonas aeruginosa*. *Biochemistry* 43(18):5239–45
100. Ouellet YH, Ndiaye CT, Gagné SM, Sebilo A, Suits MDL, et al. 2016. An alternative reaction for heme degradation catalyzed by the *Escherichia coli* O157:H7 ChuS protein: release of hematinic acid, tripyrrole and Fe(III). *J. Inorg. Biochem.* 154:103–13
101. Suits MDL, Pal GP, Nakatsu K, Matte A, Cygler M, Jia Z. 2005. Identification of an *Escherichia coli* 0157:H7 heme oxygenase with tandem functional repeats. *PNAS* 102(47):16955–60
102. Suits MDL, Jaffer N, Jia Z. 2006. Structure of the *Escherichia coli* O157:H7 heme oxygenase ChuS in complex with heme and enzymatic inactivation by mutation of the heme coordinating residue His-193. *J. Biol. Chem.* 281(48):36776–82
103. Maharshak N, Ryu HS, Fan TJ, Onyiah JC, Schulz S, et al. 2015. *Escherichia coli* heme oxygenase modulates host innate immune responses. *Microbiol. Immunol.* 59(8):452–65
104. Wyckoff EE, Lopreato GF, Tipton KA, Payne SM. 2005. *Shigella dysenteriae* ShuS promotes utilization of heme as an iron source and protects against heme toxicity. *J. Bacteriol.* 187(16):5658–64
105. Nobre LS, Seixas JD, Romão CC, Saraiva LM. 2007. Antimicrobial action of carbon monoxide-releasing compounds. *Antimicrob. Agents Chemother.* 51(12):4303–7
106. Wareham LK, Begg R, Jesse HE, Van Beilen JWA, Ali S, et al. 2016. Carbon monoxide gas is not inert, but global, in its consequences for bacterial gene expression, iron acquisition, and antibiotic resistance. *Antioxid. Redox Signal.* 24(17):1013–28
107. Alteri CJ, Mobley HLT. 2007. Quantitative profile of the uropathogenic *Escherichia coli* outer membrane proteome during growth in human urine. *Infect. Immun.* 75(6):2679–88
108. Mobley HLT. 2016. Measuring *Escherichia coli* gene expression during human urinary tract infections. *Pathogens* 5(1):7
109. Johnson JR, Owens K, Gajewski A, Kuskowski MA. 2005. Bacterial characteristics in relation to clinical source of *Escherichia coli* isolates from women with acute cystitis or pyelonephritis and uninfected women. *J. Clin. Microbiol.* 43(12):6064–72
110. Roos V, Klemm P. 2006. Global gene expression profiling of the asymptomatic bacteriuria *Escherichia coli* strain 83972 in the human urinary tract. *Infect. Immun.* 74(6):3565–75
111. White C, Yuan X, Schmidt PJ, Bresciani E, Samuel TK, et al. 2013. HRG1 is essential for heme transport from the phagolysosome of macrophages during erythrophagocytosis. *Cell Metab.* 17(2):261–70
112. Rajagopal A, Rao AU, Amigo J, Tian M, Upadhyay SK, et al. 2008. Haem homeostasis is regulated by the conserved and concerted functions of HRG-1 proteins. *Nature* 453(7198):1127–31
113. Khan AA, Quigley JG. 2013. Heme and FLVCR-related transporter families SLC48 and SLC49. *Mol. Aspects Med.* 34(2–3):669–82
114. O'Callaghan KM, Ayllon V, O'Keeffe J, Wang Y, Cox OT, et al. 2010. Heme-binding protein HRG-1 is induced by insulin-like growth factor I and associates with the vacuolar H^+-ATPase to control endosomal pH and receptor trafficking. *J. Biol. Chem.* 285(1):381–91
115. Yanatori I, Tabuchi M, Kawai Y, Yasui Y, Akagi R, Kishi F. 2010. Heme and non-heme iron transporters in non-polarized and polarized cells. *BMC Cell Biol.* 11:39
116. Davudian S, Mansoori B, Shajari N, Mohammadi A, Baradaran B. 2016. BACH1, the master regulator gene: a novel candidate target for cancer therapy. *Gene* 588(1):30–37
117. Kellogg SL, Little JL, Hoff JS, Kristich CJ. 2017. Requirement of the CroRS two-component system for resistance to cell wall-targeting antimicrobials in *Enterococcus faecium*. *Antimicrob. Agents Chemother.* 61(5):e02461-16
118. Hafer C, Lin Y, Kornblum J, Lowy FD, Uhlemann AC. 2012. Contribution of selected gene mutations to resistance in clinical isolates of vancomycin-intermediate *Staphylococcus aureus*. *Antimicrob. Agents Chemother.* 56(11):5845–51

119. Howden BP, McEvoy CRE, Allen DL, Chua K, Gao W, et al. 2011. Evolution of multidrug resistance during staphylococcus aureus infection involves mutation of the essential two component regulator WalKR. *PLOS Pathog.* 7(11):e1002359
120. Guckes KR, Breland EJ, Zhang EW, Hanks SC, Gill NK, et al. 2017. Signaling by two-component system noncognate partners promotes intrinsic tolerance to polymyxin B in uropathogenic *Escherichia coli*. *Sci. Signal.* 10(461):eaag1775
121. Pernestig AK, Melefors Ö, Georgellis D. 2001. Identification of UvrY as the cognate response regulator for the BarA sensor kinase in *Escherichia coli*. *J. Biol. Chem.* 276(1):225–31
122. Wei BL, Brun-Zinkernagel AM, Simecka JW, Prüß BM, Babitzke P, Romeo T. 2001. Positive regulation of motility and *flhDC* expression by the RNA-binding protein CsrA of *Escherichia coli*. *Mol. Microbiol.* 40(1):245–56
123. Palaniyandi S, Mitra A, Herren CD, Lockatell CV, Johnson DE, et al. 2012. BarA-UvrY two-component system regulates virulence of uropathogenic *E. coli* CFT073. *PLOS ONE* 7(2):e31348
124. Kostakioti M, Hadjifrangiskou M, Pinkner JS, Hultgren SJ. 2009. QseC-mediated dephosphorylation of QseB is required for expression of genes associated with virulence in uropathogenic *Escherichia coli*. *Mol. Microbiol.* 73(6):1020–31
125. Hadjifrangiskou M, Kostakioti M, Chen SL, Henderson JP, Greene SE, Hultgren SJ. 2011. A central metabolic circuit controlled by QseC in pathogenic *Escherichia coli*. *Mol. Microbiol.* 80(6):1516–29
126. Hurtado R, Smith CS. 2016. Hyperpolarization-activated cation and T-type calcium ion channel expression in porcine and human renal pacemaker tissues. *J. Anat.* 228(5):812–25
127. Hurtado R, Bub G, Herzlinger D. 2014. A molecular signature of tissues with pacemaker activity in the heart and upper urinary tract involves coexpressed hyperpolarization-activated cation and T-type Ca^{2+} channels. *FASEB J.* 28(2):730–39
128. He F, Yang Z, Dong X, Fang Z, Liu Q, et al. 2018. The role of HCN channels in peristaltic dysfunction in human ureteral tuberculosis. *Int. Urol. Nephrol.* 50(4):639–45
129. Ziaei S, Ninavaei M, Faghihzadeh S. 2004. Urinary tract infection in the users of depot-medroxyprogesterone acetate. *Acta Obstet. Gynecol. Scand.* 83(10):909–11
130. Matsumoto R, Otsuka A, Suzuki T, Shinbo H, Mizuno T, et al. 2013. Expression and functional role of β3-adrenoceptors in the human ureter. *Int. J. Urol.* 20(10):1007–14
131. Raz S, Zeigler M, Caine M. 1972. Hormonal influence on the adrenergic receptors of the ureter. *Br. J. Urol.* 44(4):405–10
132. Leung VY, Metreweli C, Yeung CK. 2002. Immature ureteric jet doppler patterns and urinary tract infection and vesicoureteric reflux in children. *Ultrasound Med. Biol.* 28(7):873–78
133. Thulesius O, Araj G. 1987. The effect of uropathogenic bacteria on ureteral motility. *Urol. Res.* 15(5):273–76
134. Floyd RV, Upton M, Hultgren SJ, Wray S, Burdyga TV, Winstanley C. 2012. *Escherichia coli*-mediated impairment of ureteric contractility is uropathogenic *E. coli* specific. *J. Infect. Dis.* 206(10):1589–96
135. Grana L, Kidd J, Idriss F, Swenson O. 1965. Effect of chronic urinary tract infection on ureteral peristalsis. *J. Urol.* 94(6):652–57
136. Beetz R. 2003. Mild dehydration: A risk factor of urinary tract infection? *Eur. J. Clin. Nutr.* 57:S52–58
137. Scott AM, Clark J, Del Mar C, Glasziou P, Mar C Del, Glasziou P. 2020. Increased fluid intake to prevent urinary tract infections: systematic review and meta-analysis *Br. J. Gen. Pract.* 70(692):e200–7
138. Hooton TM, Vecchio M, Iroz A, Tack I, Dornic Q, et al. 2018. Effect of increased daily water intake in premenopausal women with recurrent urinary tract infections: a randomized clinical trial. *JAMA Intern. Med.* 178(11):1509–15
139. Booth J, Agnew R. 2019. Evaluating a hydration intervention (DRInK Up) to prevent urinary tract infection in care home residents: a mixed methods exploratory study. *J. Frailty Sarcopenia Falls* 4(2):36–44
140. Johnson DE, Russell RG, Lockatell CV, Zulty JC, Warren JW. 1993. Urethral obstruction of 6 hours or less causes bacteriuria, bacteremia, and pyelonephritis in mice challenged with "nonuropathogenic" *Escherichia coli*. *Infect. Immun.* 61(8):3422
141. Romero Pérez P, Mira Llinares A. 2004. Revisión de las complicaciones de la estenosis uretral masculina [Male urethral stenosis: review of complications]. *Arch. Esp. Urol.* 57(5):485–511

142. Vasudeva P, Madersbacher H. 2014. Factors implicated in pathogenesis of urinary tract infections in neurogenic bladders: some revered, few forgotten, others ignored. *Neurourol. Urodyn.* 33(1):95–100
143. Rodrigues P, Hering F, Campagnari JC. 2014. Involuntary detrusor contraction is a frequent finding in patients with recurrent urinary tract infections. *Urol. Int.* 93(1):67–73
144. Vigil HR, Hickling DR. 2016. Urinary tract infection in the neurogenic bladder. *Transl. Androl. Urol.* 5(1):72–87
145. Edokpolo L, Stavris K, Foster H. 2012. Intermittent catheterization and recurrent urinary tract infection in spinal cord injury. *Top. Spinal Cord Inj. Rehabil.* 18(2):187–92
146. Conover MS, Flores-Mireles AL, Hibbing ME, Dodson K, Hultgren SJ. 2015. Establishment and characterization of UTI and CAUTI in a mouse model. *J. Vis. Exp.* 2015(100):52892
147. Anderson CE, Chamberlain JD, Jordan X, Kessler TM, Luca E, et al. 2019. Bladder emptying method is the primary determinant of urinary tract infections in patients with spinal cord injury: results from a prospective rehabilitation cohort study. *BJU Int.* 123(2):342–52
148. Hooton TM, Bradley SF, Cardenas DD, Colgan R, Geerlings SE, et al. 2010. Diagnosis, prevention, and treatment of catheter-associated urinary tract infection in adults: 2009 international clinical practice guidelines from the Infectious Diseases Society of America. *Clin. Infect. Dis.* 50(5):625–63
149. Heudorf U, Grünewald M, Otto U. 2016. Implementation of the updated 2015 Commission for Hospital Hygiene and Infection Prevention (KRINKO) recommendations "Prevention and control of catheter-associated urinary tract infections" in the hospitals in Frankfurt/Main, Germany. *GMS Hyg. Infect. Control* 11:Doc14
150. Dinh A, Davido B, Duran C, Bouchand F, Gaillard JL, et al. 2019. Urinary tract infections in patients with neurogenic bladder. *Med. Mal. Infect.* 49(7):495–504
151. Balsara ZR, Ross SS, Dolber PC, Wiener JS, Tang Y, Seed PC. 2013. Enhanced susceptibility to urinary tract infection in the spinal cord-injured host with neurogenic bladder. *Infect. Immun.* 81(8):3018–26
152. Coe FL, Parks JH, Asplin JR. 1992. The pathogenesis and treatment of kidney stones. *N. Engl. J. Med.* 327(16):1141–52
153. Tian Y, Cai X, Wazir R, Wang K, Li H. 2016. Water consumption and urinary tract infections: an in vitro study. *Int. Urol. Nephrol.* 48(6):949–54
154. Fernández-Rodríguez A, García-Ruiz MJ, Arrabal-Martín M, Arrabal-Polo MA, Pichardo-Pichardo S, Zuluaga-Gómez A. 2006. Papel de las tiazidas en la profilaxis de la litiasis cálcica recidivante. *Actas Urol. Esp.* 30(3):305–9
155. Tekin ALI, Tekgul S, Atsu N, Bakkaloglu M, Kendi S. 2002. Oral potassium citrate treatment for idiopathic hypocitruria in children with calcium urolithiasis. *J. Urol.* 168(6):2572–74
156. Borghi L, Meschi T, Amato F, Briganti A, Novarini A, Giannini A. 1996. Urinary volume, water and recurrences in idiopathic calcium nephrolithiasis: a 5-year randomized prospective study. *J. Urol.* 155(3):839–43
157. Curhan GC, Willett WC, Speizer FE, Stampfer MJ. 2001. Twenty-four-hour urine chemistries and the risk of kidney stones among women and men. *Kidney Int.* 59(6):2290–98
158. Barr-Beare E, Saxena V, Hilt EE, Thomas-White K, Schober M, et al. 2015. The interaction between Enterobacteriaceae and calcium oxalate deposits. *PLOS ONE* 10(10):e0139575
159. Schwaderer AL, Wolfe AJ. 2017. The association between bacteria and urinary stones. *Ann. Transl. Med.* 5(2):32
160. Li C, Wang W, Knepper MA, Nielsen S, Frøkiær J. 2003. Downregulation of renal aquaporins in response to unilateral ureteral obstruction. *Am. J. Physiol. Ren. Physiol.* 284(5):F1066–79
161. Mutig K, Paliege A, Kahl T, Jöns T, Müller-Esterl W, Bachmann S. 2007. Vasopressin V_2 receptor expression along rat, mouse, and human renal epithelia with focus on TAL. *Am. J. Physiol. Ren. Physiol.* 293(4):F1166–77
162. Bachmann S, Mutig K. 2017. Regulation of renal Na-(K)-Cl cotransporters by vasopressin. *Pflügers Arch. Eur. J. Physiol.* 469(7):889–97
163. Berry MR, Mathews RJ, Ferdinand JR, Jing C, Loudon KW, et al. 2017. Renal sodium gradient orchestrates a dynamic antibacterial defense zone. *Cell* 170(5):860–74.e19
164. Kino T, Takatori H, Manoli I, Wang Y, Tiulpakov A, et al. 2009. Brx mediates the response of lymphocytes to osmotic stress through the activation of NFAT5. *Sci. Signal.* 2(57):ra5

165. Higashihara E, Torres VE, Chapman AB, Grantham JJ, Bae K, et al. 2011. Tolvaptan in autosomal dominant polycystic kidney disease: three years' experience. *Clin. J. Am. Soc. Nephrol.* 6(10):2499–507
166. Casper J, Schmitz J, Bräsen JH, Khalifa A, Schmidt BMW, et al. 2018. Renal transplant recipients receiving loop diuretic therapy have increased urinary tract infection rate and altered medullary macrophage polarization marker expression. *Kidney Int.* 94(5):993–1001
167. Atri C, Guerfali FZ, Laouini D. 2018. Role of human macrophage polarization in inflammation during infectious diseases. *Int. J. Mol. Sci.* 19(6):1801
168. Lee JH, Jang SJ, Rhie S. 2018. Antinatriuretic phenomena seen in children with acute pyelonephritis may be related to the activation of intrarenal RAAS. *Medicine* 97(36):e12152
169. de Magalhães Sartim R, Fantinato Menegon L, Roberta de Almeida A, Rocha Gontijo JA, Boer PA. 2006. Development of hypertension in a pyelonephritis-induced model: the effect of salt intake and inability of renal sodium handling. *Ren. Failure* 28(6):501–7
170. Jacobson SH. 1987. Blood pressure regulation, peripheral renin activity and aldosterone in patients with pyelonephritic renal scarring. *Acta Physiol. Scand.* 131(2):242–48
171. Kleinewietfeld M, Manzel A, Titze J, Kvakan H, Yosef N, et al. 2013. Sodium chloride drives autoimmune disease by the induction of pathogenic TH17 cells. *Nature* 496(7446):518–22
172. Kunnen SJ, Malas TB, Semeins CM, Bakker AD, Peters DJM. 2018. Comprehensive transcriptome analysis of fluid shear stress altered gene expression in renal epithelial cells. *J. Cell. Physiol.* 233(4):3615–28
173. Sanjabi S, Oh SA, Li MO. 2017. Regulation of the immune response by TGF-β: from conception to autoimmunity and infection. *Cold Spring Harb. Perspect. Biol.* 9(6):a022236
174. Liu Y, Flores D, Carrisoza-Gaytán R, Rohatgi R. 2014. Biomechanical regulation of cyclooxygenase-2 in the renal collecting duct. *Am. J. Physiol. Ren. Physiol.* 306(2):F214–23
175. Flores D, Liu Y, Liu W, Satlin LM, Rohatgi R. 2012. Flow-induced prostaglandin E2 release regulates Na and K transport in the collecting duct. *Am. J. Physiol. Ren. Physiol.* 303(5):F632–38
176. Yang T, Liu M. 2017. Regulation and function of renal medullary cyclooxygenase-2 during high salt loading. *Front. Biosci.* 22:128–36
177. Wang Y, Xiao B. 2018. The mechanosensitive Piezo1 channel: structural features and molecular bases underlying its ion permeation and mechanotransduction. *J. Physiol.* 596(6):969–78
178. Miyamoto T, Mochizuki T, Nakagomi H, Kira S, Watanabe M, et al. 2014. Functional role for Piezo1 in stretch-evoked Ca^{2+} influx and ATP release in urothelial cell cultures. *J. Biol. Chem.* 289(23):16565–75
179. Cox CD, Bae C, Ziegler L, Hartley S, Nikolova-Krstevski V, et al. 2016. Removal of the mechanoprotective influence of the cytoskeleton reveals PIEZO1 is gated by bilayer tension. *Nat. Commun.* 7(1):10366
180. Martins JR, Penton D, Peyronnet R, Arhatte M, Moro C, et al. 2016. Piezo1-dependent regulation of urinary osmolarity. *Pflügers Arch. Eur. J. Physiol.* 468(7):1197–206
181. Dalghi MG, Clayton DR, Ruiz WG, Al-Bataineh MM, Satlin LM, et al. 2019. Expression and distribution of PIEZO1 in the mouse urinary tract. *Am. J. Physiol. Ren. Physiol.* 317:303–21
182. Evans JH, Spencer DM, Zweifach A, Leslie CC. 2001. Intracellular calcium signals regulating cytosolic phospholipase A_2 translocation to internal membranes. *J. Biol. Chem.* 276(32):30150–60
183. Nelson AL, Ratner AJ, Barasch J, Weiser JN. 2007. Interleukin-8 secretion in response to aferric enterobactin is potentiated by siderocalin. *Infect. Immun.* 75(6):3160–68
184. Bachman MA, Miller VL, Weiser JN. 2009. Mucosal lipocalin 2 has pro-inflammatory and iron-sequestering effects in response to bacterial enterobactin. *PLOS Pathog.* 5(10):e1000622